Developing Biochar-Based Catalyst for Biodiesel Production

Amir Mehdi Dehkhoda

University of British Columbia

CHBE 599

August 01, 2010

Developing Biochar-Based Catalyst for Biodiesel Production

by

Amir Mehdi Dehkhoda

B.Sc., Sharif University of Technology, 2008

A THESIS SUBMITTED IN PARTIAL FULFILLMENT

OF THE REQUIREMENTS FOR THE DEGREE OF

MASTER OF APPLIED SCIENCE

in

The Faculty of Graduate Studies

(Chemical and Biological Engineering)

THE UNIVERSITY OF BRITISH COLUMBIA

(Vancouver)

August 2010

Abstract

A biochar-based catalyst was successfully prepared by sulfonation of pyrolysis char with fuming sulphuric acid. Prepared catalyst was studied for its ability to catalyze transesterification of vegetable oils (i.e., Canola Oil) and esterification of free fatty acids (i.e., oleic acid) using methanol. Thus far, biochar-based catalyst has shown significant activity, >90% conversion, in esterification of FFAs while indicating limited activity for transesterification of triglyceride-based oils such as Canola Oil. The first step in catalyst development approach was to increase the transesterification activity through employing a stronger sulfonation procedure. The total acid density of the biochar-based catalyst increased by ~90 times resulting in significantly increased transesterification yield (i.e., from being almost negligible to ~9%). Further investigations on the biochar-based catalyst were conducted to determine the effect of sulfonation time (5 and 15 h) and surface area on the transesterification reaction. Two established activation techniques (i.e., chemical activation with KOH and the silica template method) have been utilized to develop the surface area and porosity of the biochar supports. The surface area of the biochar support increased from a typical 0.2 m^2/g to over 600 m^2/g. In the chemical activation method with KOH, the effect of activation temperature on the transesterification yield has been investigated. Three biochar-based catalysts with activated supports at three different temperatures (450, 675 and 875°C) were prepared and compared for transesterification activity. The sulfonated catalysts were characterized using the following analyses: BET surface area, elemental analysis, total acid density, Fourier Transform Infra-Red (FT-IR) spectroscopy, and X-Ray Diffraction

(XRD) spectroscopy. The catalyst supported on biochar activated at 675°C resulted the maximum transesterification yield (18.9%). The reaction yield was dependent on both catalyst surface area and total acid density. The catalytic activity of the biochar-based catalyst with activated support at 675°C remained significantly high for esterification of FFAs (conversion>97%).

The structural study of the catalysts prepared from activated biochars at three different temperatures suggest that the higher activation temperatures cause an increasing re-orientation of the biochar's carbon sheets towards a more graphite-like structure, causing a decrease (> 60%) in total acid density despite of the increase in surface area.

Preface

Another version of Chapter Four, Section 4.2.2 of this thesis has been published in the *Journal of Applied Catalysis A: General*[1]. Mr. Alex H. West and Dr. Naoko Ellis have contributed as co-authors in the aforementioned publication. Experimental design of catalytic runs, conducting experiments, and compiling the data and results regarding the catalytic performance and catalyst characterization along with writing and revising the manuscript have been done by the first author. Moreover, another version of Sections 4.2.3 and 4.5 is ready to be submitted for publication. The contribution to the mentioned manuscript is as co-author. Ms. Joyleene Yu is the first author. Dr. Naoko Ellis has also contributed as the co-author. Conducting experiments, compiling the data and results have been done by the author of this thesis. Writing the manuscripts and interpretation of results have been done by the first author, Ms. Joyleene Yu.

---

[1] Dehkhoda, A.M., West, A.H. & Ellis, N., 2010. Biochar based solid acid catalyst for biodiesel production. Applied Catalysis A: General, 382(2), 197-204

Table of Contents

List of Tables

List of Figures

Nomenclature

A:O- Alcohol to Oil

Ar-OH- Aromatic phenolic

ASTM- American Society for Testing and Materials

ATR- Attenuated Total Reflectance

BET- Brunauer, Emmett and Teller

BJH- Barrett, Joyner and Halenda

C(002)- Specific diffracting plane in carbon structure for XRD analysis

C(101)- Specific diffracting plane in carbon structure for XRD analysis

C:18- Fatty acid with 18 carbon atoms

C-(450, 675, 875°C)- Activated biochar samples at (450, 675, 875°C)

C-(450, 675, 875°C)-SO_3H- Sulfonated Activated biochar samples at (450, 675, 875°C)

C=O- Carbon bonded oxygen (double bond)

CAM- Chemical Activation Method

CO- Carbon monoxide

CO_2- Carbon dioxide

FFA- Free Fatty Acid

FT-IR- Fourier Transform Infra Red

GC- Gas Chromatography

GC/MS- Gas Chromatography Mass Spectroscopy

H/C- Hydrogen to Carbon ratio

HCL- Hydrochloric Acid

HF- Hydrofluoric Acid

H-NMR- Proton Nuclear Magnetic Resonance

HP- Hewlett Packard

MAWP- Maximum Allowable Working Pressure

MOH- Alkali Hydroxide (e.g., Potassium (K), Sodium (Na))

MO- Methyl Oleate

MLO- Methyl Linoleate

M_2CO_3- Alkali Carbonate

O/C- Oxygen to Carbon ratio

PSD- Pore Size Distribution

R- Alkyl group

ROH- Alcohol

RPM- Round Per Minute

S=O- Sulphur bonded oxygen (double bond)

SO_3- Sulphur Trioxide

SO_3H- Sulfonic group

STM- Silica Template Method

TEOS- Tetraethyl Orthosilicate

TG- Triglyceride

UBC- University of British Columbia

WVO- Waste Vegetable Oil

XRD- X-Ray Diffraction

$ZnCl_2$- Zinc Chloride

λ- Wavenumber (cm^{-1})

θ– Bragg Angle (°)

Acknowledgments

I would like to express my gratitude to my supervisor, Dr. Naoko Ellis, who provided me with this incredible opportunity to come to UBC and be a part of her research group. Her support, patience, and constant guidance helped me through overcoming many of the challenges that I faced during my studies.

I would like to acknowledge Dr. P. B. Fransham and Dr. S. Duff for reviewing my thesis and being a part of my research committee. Dr. Fransham went beyond the call of duty by both providing his comments and suggestions, and also supplying the biochar material during the project.

In the last 6 months of my program, I received an incredible help from Joyleene R. Yu during her co-op program at UBC. She helped me enormously through conducting of experiments and data collection. Her hard work, desire to learn, and kind friendship are greatly appreciated.

I also want to express my debt to my research mates. I would like to thank Jidon Janaun, Masakazu Sakaguchi, Soojin Lee, and Steve Reaume for all their help and cooperation. I have had an excellent experience in both research work and friendship with all of them.

I also want to thank Dr. Kevin Smith and Dr. Madjid Mohseni from Department of Chemical and Biological Engineering for letting me use their laboratories and equipments. My special thanks also go to Mr. Tim Ma from Department of Civil

To my beloved parents and sister

1. Introduction

1.1 Background

Concerns over diminishing fossil fuel reserves, rising oil prices, and environmental impacts, have all contributed to the large research efforts made to develop and secure renewable energy sources such as biofuels. Biodiesel, mono-alkyl esters of long chain fatty acids, is one of the promising alternatives (or extenders) to conventional petroleum based diesel fuel. This alternative source of energy has a number of advantages including, but not limited to, being renewable, environmental benign, having less CO_2 emissions on life cycle analysis basis, and lower toxicity. However, the large scale biodiesel production is associated with challenging issues such as high cost of production and affecting the food supply by using edible oils as feedstock.

Biodiesel can be produced through transesterification of vegetable oils or esterification of Free Fatty Acids (FFAs). In 1853, many years before the invention of the first diesel engine, vegetable oil transesterification was carried out by scientists E. Duffy and J. Patrick (Kirakosyan & Kaufman 2009). In 1900, Rudolf Diesel operated his engine with peanut oil at the Paris exhibition (Canakci & Sanli 2008). During the 1920s and 1930s several countries such as Germany, United Kingdom, Japan, and China started initiatives to test and use vegetable oils as fuel in internal combustion engines. Later, during World War II, vegetable oils were used as a diesel fuel but the practise was abandoned due to the availability of inexpensive petroleum fuel (Knothe 2001). The high viscosity and low volatility of vegetable oils were also problematic for use in diesel

engines, though these issues were reduced in the years that followed (Goering et al. 1981; Demirbas 2003). The onset of the oil crisis in 1970 led to an increase in research on the usage of vegetable oils in diesel engines once again. According to the International Energy Agency (IEA) biofuel production rapidly increased in the past few years. As shown in Figure 1.1, global biodiesel production increased from almost 2 to 15 billion litres in the period of 2005 to 2008 (IEA 2009). Nevertheless, there are still two main drawbacks for the large scale biodiesel production; high cost and food crisis issue. The high cost of biodiesel production is mainly attributed to the cost of fresh vegetable oil feedstock (Canakci & Van Gerpen 2001). Moreover, the competition of fresh vegetable oil as a major feedstock for large scale biodiesel production with food source has driven up the food prices, especially in recent years, leading to potentially reducing the access of food to vulnerable communities around the world (Escobar et al. 2009).
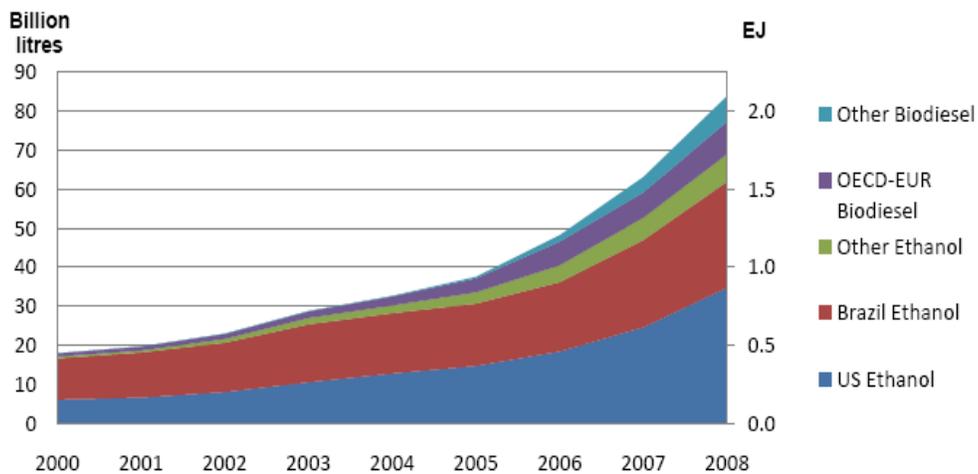
Figure 1.1. Global biofuel production 2000-2008 (IEA 2009)

One of the proposed solutions for the aforementioned drawbacks of biodiesel production is using alternative cheap feedstock such as Waste Vegetable Oil (WVO)

instead of fresh vegetable oil. Approximately 15 million tons of WVOs are generated annually from the restaurants and households just in the United States, China, and Malaysia (Gui et al. 2008). The disposal of WVOs, if treated as waste, may cause blockage and odour problems while discharging into the drains and sewers, thus, using WVOs as a feedstock would have the added benefit of reducing disposal problems. However, using this kind of feedstock is challenging due to the presence of higher contents of Free Fatty Acids (FFAs) in addition to the Triglycerides (TGs). The higher amount of FFAs interferes with transesterification (in the presence of an alkali catalyst) resulting in the formation of unwanted soap by-product which requires expensive separations (Zong et al. 2007). Therefore, biodiesel production from WVOs feedstock should be conducted in a two-step process including the conversion of FFAs to corresponding esters in the first step, and the conversion of the remaining Triglycerides (TGs) to alkyl esters, i.e., biodiesel, in the second step (Nakajima et al. 2007; Zong et al. 2007). As shown in Figure 1.2, each step requires different catalyst in addition to costly washing and neutralization operations. However, in the presence of a solid catalyst, i.e., heterogeneous catalyst, the two-step production can be conducted in one step while further washing and neutralizations be eliminated (shown in Figure 1.3). Ease of separation and being cheaply available are among the other advantages of the solid catalyst such as amberlyst, zeolites and niobic acids. Moreover, the use of heterogeneous catalysts is reported to be the most economically viable process in a comparison of main four large scale continuous biodiesel production processes from WVO feedstock (West et al. 2008). Therefore, developing a promising bi-functional solid

acid catalyst for simultaneous transesterification of TGs and esterification of FFAs from

WVOs feedstock is a crucial step in the commercialization of biodiesel production.
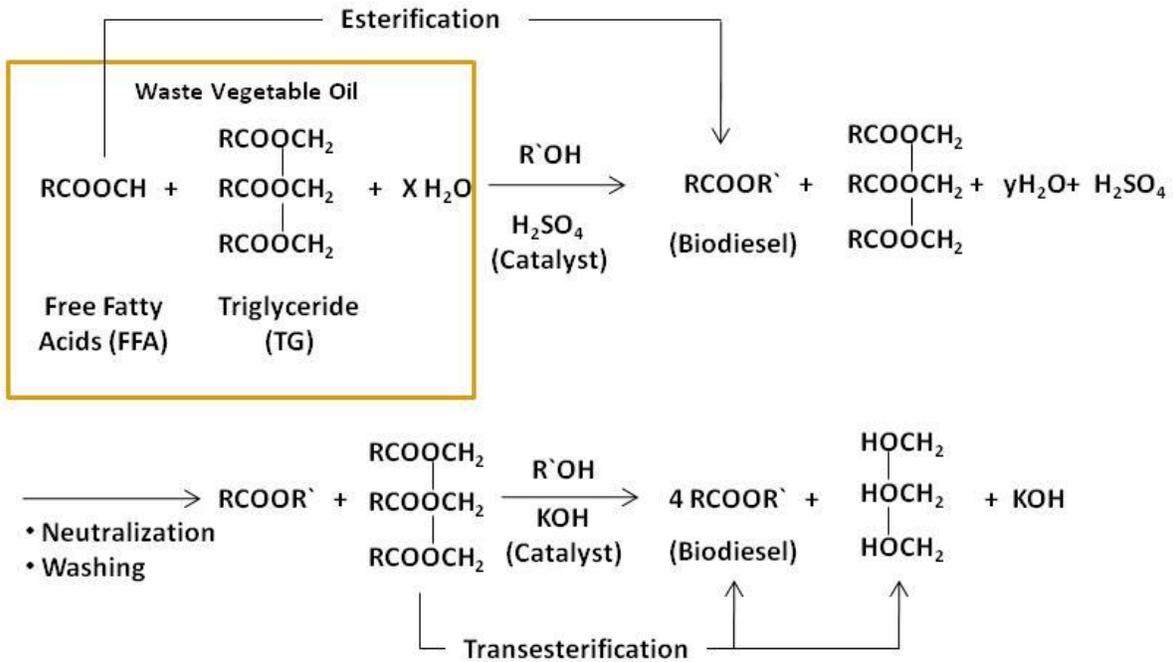
Figure 1.2. Two step biodiesel production from Waste Vegetable Oil feedstock (Adopted from Nakajima et al. 2007)
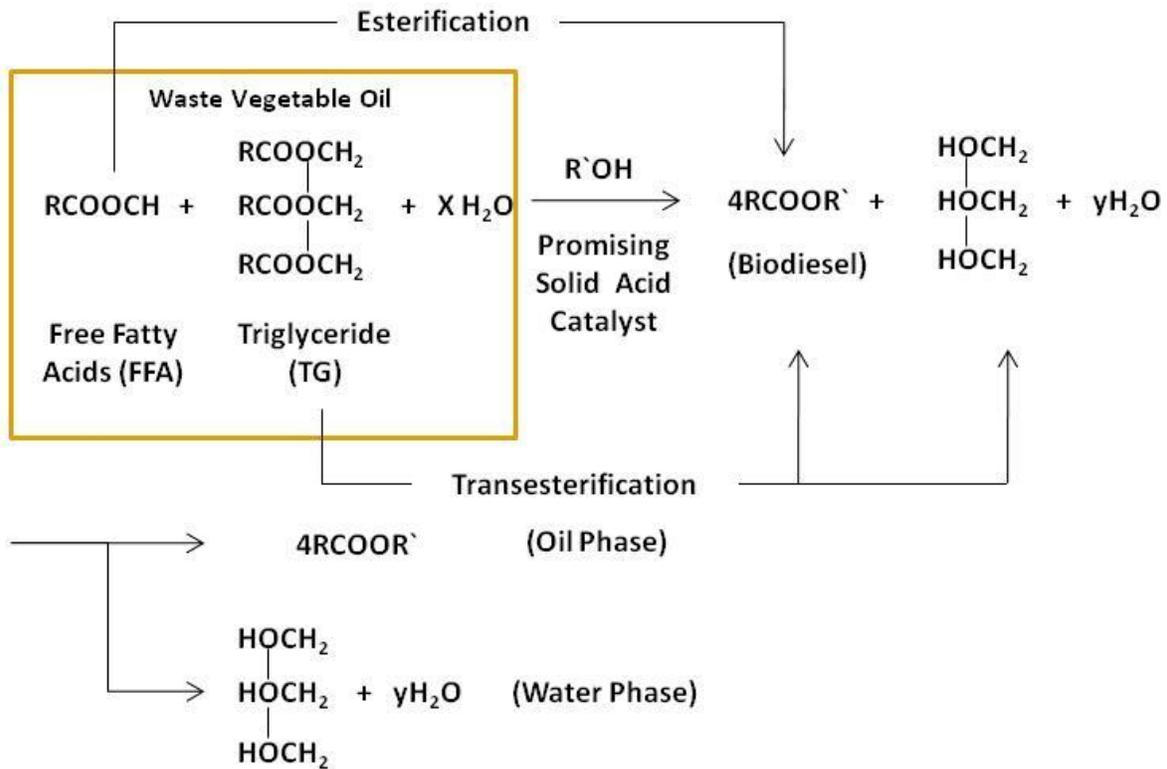
Figure 1.3. One step biodiesel production from Waste Vegetable Oil feedstock in the presence of promising catalyst Adopted from (Nakajima et al. 2007)

1.2   Research Objectives

This study explores the potential application of biochar as a heterogeneous catalyst support bearing sulfonic groups for biodiesel production from WVO feedstock. The main objective is to develop a promising solid acid catalyst supported on a novel carbon-based material with catalytic abilities for both transesterification of TGs and esterification of FFAs. Biochar is one of the by-products of the conventional pyrolysis of woody biomass (to produce bio-oil) which is commercially utilized for soil amendment and carbon sequestration (Mohan et al. 2006). Using biochar-based catalyst for

biodiesel production would have the added benefit of increasing the environmental viability of bio-oil production via pyrolysis process.

The catalyst development has focused on two main aspects: stronger functionalizing, i.e., sulfonation, and development of the surface area and porosity of the biochar support. The latter procedure has been conducted via two techniques namely chemical activation with KOH and the silica template method. Transesterification of canola oil and esterification of oleic acid (as a model compound) using methanol as an alcohol reagent are the main reactions involved in this study for catalytic activity comparisons.

The main objectives of the present study are:

- Analyzing the effect of stronger functionalization, i.e., sulfonation, on transesterification activity of biochar-based catalyst;

- Investigation the effect of different activation methods on the development of surface area and porosity of biochar support;

- Analyzing the effect of biochar activation temperature on the transesterification activity of biochar-based catalysts;

- Structural study of the biochar-based catalysts with supports prepared at three different activation temperatures;

- Testing the esterification activity of the best biochar catalyst based on the highest transesterification yield;

- Preparation and testing of catalysts supported on different biochar samples pyrolyzed from various feedstock such as corn stover; and

- Examine the effect of higher temperature/pressure on the transesterification activity in autoclave reactor.

1.3 Thesis Format

The remainder of this thesis continues with four chapters. **Chapter Two** reviews the published literature survey regarding the catalyst utilization for biodiesel production. The most commonly used catalysts and the new generation of carbon-based catalysts for biodiesel production have been compared and reviewed. In the following the introductory literature survey based on the methods of surface area and porosity development and their applications for carbon based material is presented. In **Chapter Three**, the experimental methods, apparatus, and the characterization techniques have been explained. **Chapter Four** includes the results and discussions of the porosity development methods, catalytic activity comparisons, and the structural study of the prepared catalysts. Finally the thesis is concluded in **Chapter Five** with the general discussion of the results and the recommendations for future research. This thesis is written in the traditional format. The following publications have been made from another version of the mentioned sections of this thesis:

- Chapter Four, Section 4.2.2 is published in the *Journal of Applied Catalysis A: General.*[1]
- Chapter Four, Sections 4.2.3 and 4.5 to be submitted to journal of *Energy & Fuels.*[2]

---

[1]Dehkhoda, A.M., West, A.H. & Ellis, N., 2010. Biochar based solid acid catalyst for biodiesel production. *Applied Catalysis A: General*, 382(2), 197-204.

[2] Yu, J.R., Dehkhoda, A.M. & Ellis, N., Effect of Char Activation Temperature on Transesterification Activity of Biochar-based Catalysts, to be submitted to journal of *Energy & Fuels.*

2. Literature Review

2.1 Commonly Used Catalysts for Biodiesel Production

The commonly used catalysts for biodiesel production can be categorized into four main groups including homogeneous alkalis such as potassium hydroxide, homogeneous acids such as sulfuric acid, enzymes such as lipases, and heterogeneous acid catalysts such as sulfated zirconia (Zong et al. 2007). Using the homogeneous alkali catalysts is the most common and well known industrial method for biodiesel production (Zhang et al. 2003). However, this type of catalyst is generally corrosive to equipment and reacts with the large amount of Free Fatty Acids (FFAs) in the WVO feedstock to form unwanted by-products such as soaps (as mentioned in Section 1.1) (Zong et al. 2007). The next group of commonly used catalysts, homogeneous acid catalysts, are disadvantageous because of their contribution to corrosion and environmental problems requiring more expensive equipment. Enzyme based catalysts are generally too expensive and cause further problems in the presence of FFAs and short chain alcohols, even though they are non-polluting and effective catalysts (Zong et al. 2007). However, the heterogeneous solid acid catalysts showed a number advantages comparing to the rest of commonly used catalysts, such as having the most economical biodiesel production process and ease of separation and reusability (Lotero et al. 2005). There are a number of reported heterogeneous solid acid catalysts for biodiesel production such as strong acidic ion exchange resins (e.g., amberlyst), inorganic-oxide solid acids (e.g., zeolite and niobic acids), and sulfated zirconia, all of which are either too expensive, or too weak in the sense of effective acid sites and catalytic activity (Harmer et al. 1998; Bossaert et al. 1999; Okuhara 2002; Kiss et al. 2006). The carbon-

based solid acid catalysts recently showed higher activity for esterification and transesterification reactions comparing to other solid acid catalysts such as sulphated zirconia, amberlyst, niobic acid, and Nafion (Table 2.1).

Table 2.1. Different solid acid catalysts used for transesterification/esterification reactions

Catalyst	Reaction			Yield (%)	Reference
	Type	Temperature (°C)	Time (h)		
Sulphated Zirconia	Transesterification/ Esterification[1]	80	9	63	(Zong et al. 2007)
Amberlyst-15				33	
Niobic Acid				10	
Carbon-Based				85	
Nafion SAC-13	Transesterification[2]	60	1	72	(Mo et al. 2008a)
	Esterification[3]			30	
Carbon-Based	Transesterification[2]	60	1	91	
	Esterification[3]			41	

2.2 Carbon-Based Solid Acid Catalyst

The development of solid acid catalysts has recently gained attention due to their lack of corrosion and toxicity problems, as well as ease of separation compared to other reported catalysts for biodiesel production (Clark 2002; Okuhara 2002). In the solid acid catalyst group, considerable efforts have been made to develop carbon based solid acid catalysts from D-glucose material, called "Sugar Catalyst", as highly active and stable

---

[1] WVO with 27.8% FFA used as feedstock
[2] Transesterification of triacetin
[3] Esterification of acetic acid

reagents for biodiesel production. These materials have lower production cost compared to other solid acid catalysts such as strong acidic cation-exchangeable resins, i.e. nafion (Okamura et al. 2006; Nakajima et al. 2007; Zong et al. 2007; Mo et al. 2008b). D-glucose based solid acid catalyst was first reported by Toda et al. (2005) for esterification of long chain fatty acids to produce biodiesel. Zong et al. (2007) extended Toda`s study to the reactivity of carbon based solid acid catalyst for more than fifty cycles of successive re-use and have briefly reviewed the advantages and disadvantages of "Sugar Catalyst" for biodiesel production. Structural, physical and chemical characterization, catalytic activity, stability and application of "sugar catalyst" have been reported to be superior to the other solid acid catalysts such as sulphated zirconia and Niobic acid (Zong et al. 2007). In the same year, another group of researchers have studied amorphous carbonized D-glucose at temperatures ranging between 573 and 823 K bearing sulfonic acid groups as a promising catalyst for biodiesel production (Nakajima et al. 2007). In the mentioned temperature range, sulfonation of carbonized material (i.e., from sugar) at > 723 K did not produce an active catalyst due to the "rigidity" of the supporting material (Nakajima et al. 2007). According to Nakajima et al. (2007), a determining factor on catalytic activity of sulfonated carbon catalysts is the pyrolysis temperature of the supporting material.

Mo et al. (2008b) reported on a novel sulfonated carbon composite solid acid catalyst which was derived from the pyrolysis of a polymer matrix impregnated with glucose. This novel catalyst has higher esterification activity, higher acid site densities, and better reusability than the previously reported "sugar catalyst". However, the surface area of

the newly developed sugar catalyst on polymer matrix did not exceed 1 m^2/g in spite of being supported on a porous media.

The activation/deactivation characteristics of the "sugar catalysts" with pyrolyzed D-glucose support at 350 and 400°C and three various pyrolysis times have been investigated by (Mo et al. 2008a). H-NMR (Proton Nuclear Magnetic Resonance) and elemental analysis of fresh and used catalysts were used to investigate catalyst deactivation which was mainly caused by leaching of polycyclic aromatic hydrocarbons containing SO_3H group. Active site leaching of catalyst in solvents other than methanol such as water, ethanol and hexane is one of the contrary results compared to previous studies, e.g., Okamura et al. (2006) and Nakajima et al. (2007). Also, the activity may decrease or increase during consecutive reactions due to the molecular size and hydrophobicity of free fatty acids or triglycerides which was again in contrast with the previously reported results, e.g., Zong et al. (2007).

The acid density and strength of the sulfonated D-glucose based catalysts and the catalytic activities are summarized in Table 2.2. The first line shows the carbon char without any sulfonation; while the second line is the pure sulphuric acid – representing two extreme cases of acid density for comparison. It is shown that the surface area is not necessarily correlated well with the catalytic activity. All prepared carbon catalysts have shown comparable activity to that of sulphuric acid for both transesterification and esterification reactions. The sulfonated carbon composite introduced by (Mo et al. 2008b), showed higher acid site density and better fatty acid esterification activity with the same value of surface area (<1 m^2/g) among the others owing to the presence of much higher acid site densities.

Table 2.2. Reported data for carbon-based solid acid catalyst in the literature

Catalyst	Carbon support	Surface area, (m²/g)	Acid density, mmol/g		Acidity	Formation rate, µmol/min	Reference
			Total	SO₃H			
Carbon (D-glucose char) without sulfonation	D-glucose char	< 1	0.2	0	-	Acetic acid conv. (1h) < 1	(Mo et al. 2008a)
H₂SO4	-	-	20.4	N/A[1]	-	156 (ethyl oleate)	(Toda et al. 2005; Takagaki et al. 2006)
Carbon (Concentrated H₂SO₄)	D-glucose char	2	1.4	0.7	-11<pKa<-8	44 (ethyl oleate)	(Toda et al. 2005; Takagaki et al. 2006)
Carbon (fuming H₂SO₄)	D-glucose char	1	2.5	1.2	-11<pKa<-8	86 (ethyl oleate)	(Toda et al. 2005; Takagaki et al. 2006)
Carbon (Concentrated H₂SO₄)	D-glucose char	2	N/A	0.75	-11<pKa<-8	Yield of DMB[2] = 3.0% Rate ethyl acetate = 1.36 mmol/g.min	(Okamura et al. 2006)
Carbon (fuming H₂SO₄)	D-glucose char	2	N/A	1.34	-11<pKa<-8	Yield of DMB = 4.5% Rate ethyl acetate = 2.20 mmol/g.min	(Okamura et al. 2006)
Carbon (H₂SO₄)	D-glucose char	4.13	N/A	N/A	-	67 (Methyl oleate) Biodiesel yield > 90%	(Zong et al. 2007)
Carbon (H₂SO₄)	D-glucose char	< 1	-	0.60	-	Acetic acid conv.(1h): 39.7	(Mo et al. 2008a)
Carbon (H₂SO₄) – 1 hr pyrolysis	D-glucose char	< 1	3.7	0.64	-	Acetic acid conv. (1h): 42.7	(Mo et al. 2008a)
Composite (Polymer-Carbon) (H₂SO₄)	D-glucose char	< 1	N/A	2.42	-	Acetic acid conv. (1h): 72.4	(Mo et al. 2008b)

---

[1] Not Available

[2] DMB – 2, 3-dimethyl-2-butanol

2.3 Biochar-Based Solid Acid Catalyst

Biochar, a by-product from biomass pyrolysis process, is another potential carbon source to be used as a support for solid acid catalyst. Pyrolysis of agricultural waste is one of the promising thermo-chemical methods to produce bio-oil, biochar and combustible gases. The fast pyrolysis process typically yields up to 75wt% bio-oil as its main product, and the non-condensable gases (10-20 wt%) and the biochar (15-25 wt%) as by-products (Mohan et al. 2006). Numerous recent studies (Sipilae et al. 1998; Demirbas & Arin 2002; Luo et al. 2004; Yaman 2004; Mohan et al. 2006) have focused on the utilization of these products, but biochar has received very little attention. As the main scope of this thesis, the upgrading of biochar as a value added catalyst is investigated in order to increase both the environmental and economical viability of the biomass pyrolysis process. A preliminary study has confirmed the effectiveness of sulfonated biochar as catalyst for esterification of fatty acids in the biodiesel production (West 2006). However, the biochar-based catalyst showed poor activity for transesterification of canola oil even at considerably long reaction time, i.e., 24 hours. To the best knowledge of the author, the biochar-based catalyst is a novel catalyst for biodiesel production. The biochar-based catalyst is prepared through sulfonation of as-received biochar material under inert gas. Three acidic groups of sulfonic, carboxylic, and phenolic have introduced into the carbon matrix due to sulfonation. Among all mentioned groups, the sulfonic group contributes much to transesterification and esterification reactions due to higher acidic strength (Mo et al. 2008a).

The biochar-based support is believed to be consisted of amorphous polycyclic aromatic carbons sheets similar to what have been reported for the sugar catalyst (Toda et al. 2005; Okamura et al. 2006; Nakajima et al. 2007). The atomic number of carbon is six and its electron configuration in the ground state is $1s^2$, $2s^2$, $2p^2$. Carbon can bond to itself (i.e., catenation) via two hybridizations of sp^3 (diamond-like) and sp^2 (graphite-like) (Patrick 1995). In the sp^2 hybrid each carbon atom within a sheet (layer) is bonded to three adjacent carbon atoms which are directed at 120° to each other. The fourth electron of each carbon atom is capable of participating in π-bonds with neighbouring atoms (Marsh et al. 1997). The carbon sheets are parallel and are held together by weak Van der Waals forces.

The perfect graphite is a rare form of carbon since the majority of the carbon material has less ordered structures such as chars, cokes and coals. The general classification of carbon materials is shown in Figure 2.1. Basically the carbon based material can be classified into two groups of graphitic and non-graphitic carbons depending on the degree of crystallographic ordering (Marsh et al. 1997): In graphitic carbons a three-dimensional hexagonal crystalline long-range order can be detected by the typical diffraction methods, whereas, the non-graphitic carbons do not possess them (McNaught & Wilkinson 1997; Marsh 2001); while, the non-graphitic group are categorized into two further groups of graphitizable and non-graphitizable (Franklin 1951; Patrick 1995; Marsh et al. 1997). Graphitizable carbons are mainly non-graphitic carbon materials which can be converted to graphitic carbons by heat treatment. Heat Treatment Temperature (HTT) and the corresponding residence time at HTT are two

main factors affecting the degree of graphitization (Marsh 2001). On the other hand, non-graphitizable carbons do not turn into graphitic carbons even at temperatures as high as 2500°C. The graphitizable carbons, called cokes, are commercially formed from pyrolysis of coal-tar pitches and aromatic petroleum. Carbonization products from wood, activated carbons, highly volatile bituminous, brown coals, and lignite constitutes non-graphitizable carbons, called chars. Thus, biochar basically is classified as non-graphitic, non graphitizable carbons.
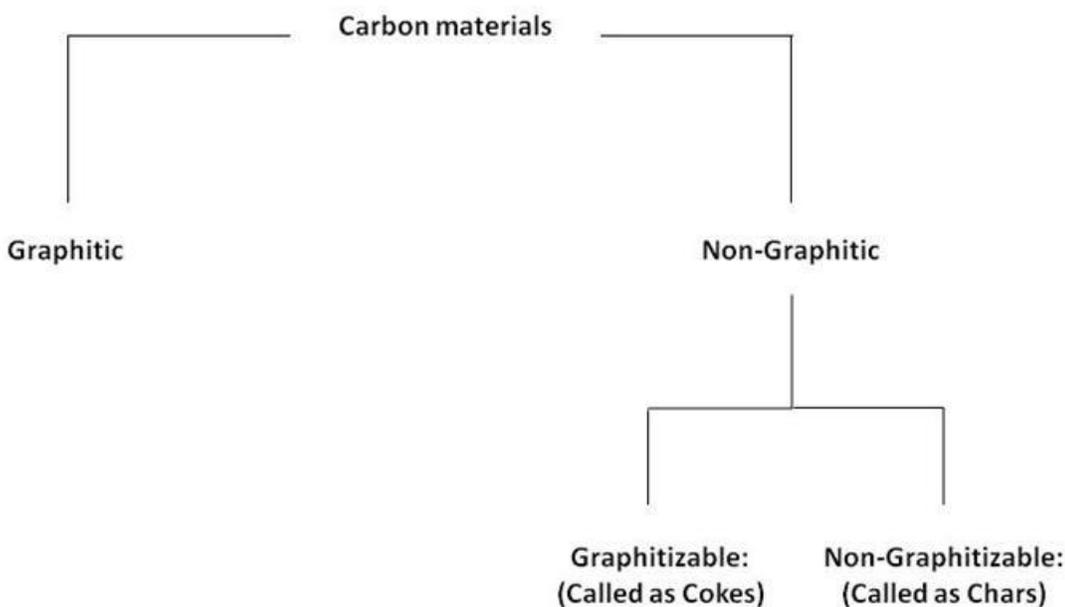
Figure 2.1. Schematic classification of carbon materials (Adopted from Patrick, 1995).
Biochar support consists of carbon sheets including polycyclic aromatic rings (Lehmann & Joseph 2009). Three different acidic groups of phenolic, carboxylic, and sulfonic are attached to the carbon atoms at the edge area of each carbon sheet after sulfonation as shown in Figure 2.2. The mentioned edge area of carbon sheets contain unsaturated

carbon atoms which are associated with high concentrations of unpaired electrons and consequently play an important role in chemisorptions (Marsh et al. 1997).

: SO$_3$H
: COOH
: OH
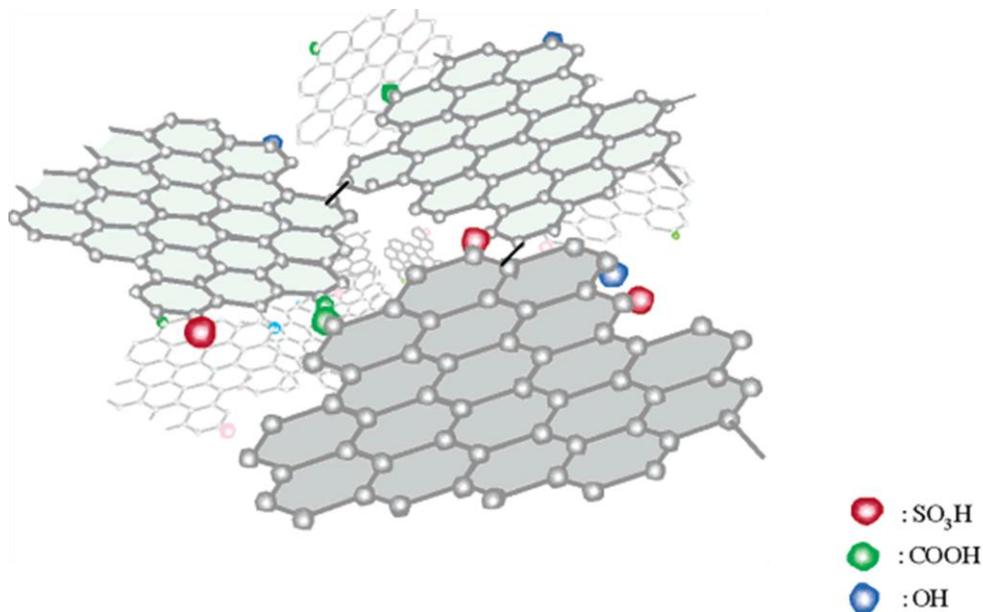
Figure 2.2. Structure of biochar-based catalyst (Okamura et al. 2006)

Biochar is categorized as non-graphitic/non-graphitizable carbons (Lehmann & Joseph 2009). By increasing the activation temperature, the structure of biochar becomes ordered to a certain extent, but not to the extent of completely ordered structure of graphitic carbons. Hence, an ordered porous carbon structure is formed by increasing the activation temperature. Biochar materials have a special state of crystalline disorder known as turbostratic wherein the successive layer planes (i.e., carbon sheets) are arranged approximately parallel and equidistant, but rotated randomly to each other (Ertl et al. 1999; Lehmann & Joseph 2009). There is no measurable crystallographic order in the direction perpendicular to carbon sheets unlike that of graphitic structures (Figure 2.3). This kind of disordering results in the absence or broadness of typical

graphitic X-Ray Diffraction (XRD) patterns as will be discussed further in this section (Ertl et al. 1999).
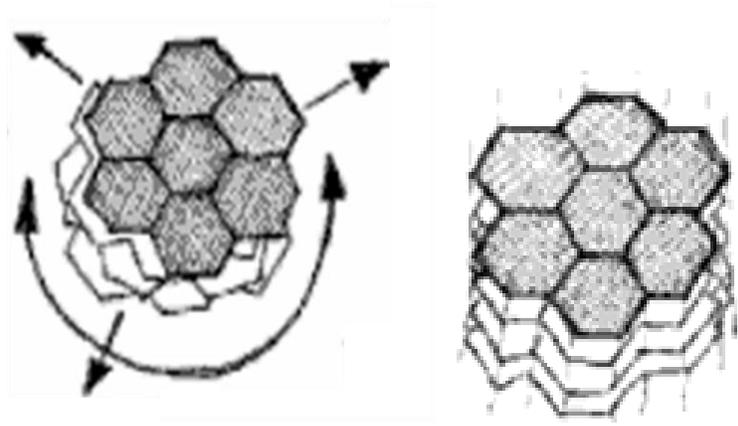
Figure 2.3. Turbostratic arrangement (left) and graphitic arrangement (right) of carbon sheets (Lehmann & Joseph 2009)

According to (Franklin 1951), the non-graphitic/non-graphitizable structures contain different parallel groups of carbon sheets which are strongly cross linked together as shown in Figure 2.4. By increasing the carbonization temperature (e.g., up to 1500°C), the cross-links begin to break, while the carbon layers set free, and be severely compressed by the surrounding cross-linked structures to form more ordered structures. Simultaneously, by increasing the activation temperature (e.g., up to 1500°C), more heteroatoms will be removed from carbon sheets leaving free carbon radicals behind (Pierson 1993). These radicals attach to each other to produce larger carbon sheets. Consequently, more ordering will happen within the interior of solid material through increasing the temperature (e.g., up to 1500°C) known as "localized crystallization" (Franklin 1951). However, by further increasing the temperature (e.g., up to 2500°C), this mechanism will cease mainly due to the disruption of surrounding cross-linked structures and a significant reduction in the amount of tension within the network

(Franklin 1951). On the other hand, at low carbonization temperatures (e.g., 350°C), the neighbour groups of carbon layers do not stack together to generate larger carbon layers and a lower percentage of heteroatoms would be removed from carbon network, consequently, generating less order in the carbon structure.
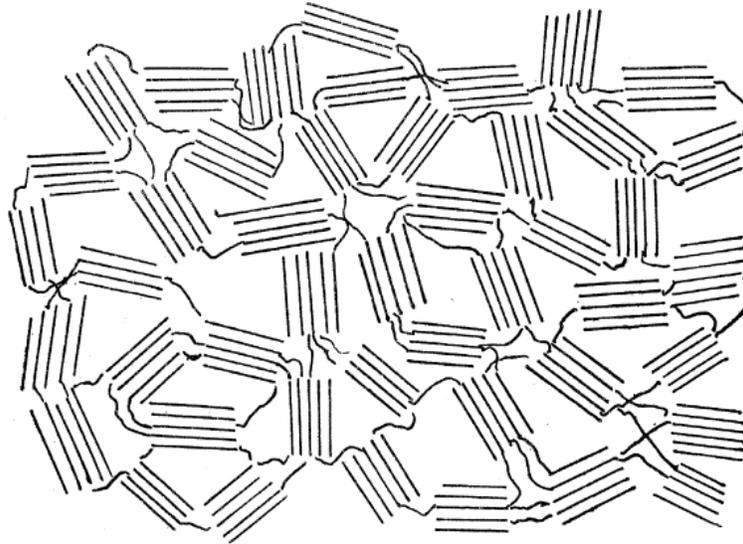
Figure 2.4. The structure of non graphitizable carbons (Franklin 1951)

2.4   Porosity Development in Carbon-Based Material

There is a need to improve the porosity and surface area of carbon-based material (e.g., biochar) for different applications such as catalysis. The following sections provide the literature to support the frequently used methods to develop the surface area and porosity of carbon-based material. Porosity is basically composed of volume elements, i.e., pores, within a solid material (Marsh 2001). In a porous carbon material the spaces between the crumpled carbon sheets constitute the porosity as shown in Figure 2.5 (Rodríguez-Reinoso & Molina-Sabio 1998). Carbons have lots of diversity in the number of different Pore Size Distributions (PSD) (Marsh 2001). Their PSDs can be modified

through different techniques for different applications. The nomenclature for describing size ranges of porosity can be categorized as follow (Marsh 2001):

- Ultra-microporosity: < 0.5 nm diameter

- Microporosity 0.5 to 2.0 nm diameter

- Mesoporosity 2.0 to 50 nm diameter

- Macroporosity >50 nm diameter

The free spaces between the crumpled carbon sheets, i.e., pores, can be filled or blocked by tarry products evolving during the pyrolysis (Rodríguez-Reinoso & Molina-Sabio 1998). There are a number of methods for synthesizing porous carbon material through chemical and physical activation methods. The mechanism of the chemical activation method is not well understood; however, it is believed that chemical activation mainly involves modifying the pyrolysis chemistry (e.g., using zinc chloride or phosphoric acid as dehydrating agents during the carbonization process) to generate different PSDs (Marsh 2001). Further modifications of the generated PSDs can be done via Physical Activation. Physical activation method is conducted mainly through gasification with steam, carbon dioxide, air or a combination of these reagents which removes carbon atoms from the walls of the original porosity. Another commonly used technique to synthesize porous carbon material is silica template method (Hu et al. 2006). This technique mainly involves two steps including infiltration of carbon precursor into pre-formed silica template followed by carbonization of the precursor and removal of the template.
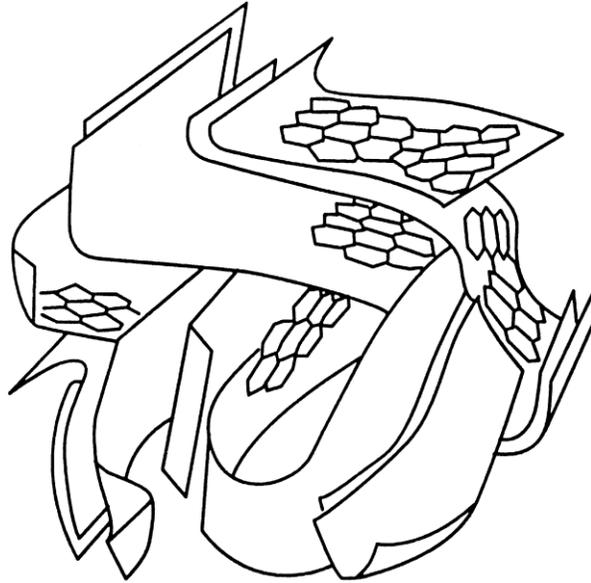
Figure 2.5. Schematic representation of a porous carbon material
(Rodríguez-Reinoso & Molina-Sabio 1998)

2.4.1 Chemical activation

According to the literature, carbonization of pre-treated precursors with chemicals such as phosphoric acid, potassium hydroxide and zinc chloride is called chemical activation (Rodríguez-Reinoso & Molina-Sabio 1998; Khalili et al. 2000; Ahmedna et al. 2000; Lillo-Ródenas et al. 2003; Hu et al. 2006). In this way, the aforementioned chemicals restrict the formation of tars in carbon networks during the pyrolysis. Table 2.3 shows steps involved with chemical activation method.

Table 2.3. Chemical activation steps reported in the literature

Chemical activation approach	1st step	2nd step	3rd step	4th step	5th step	6th step	7th step
(Chen et al. 2002)	Raw material (sludge) dried at 103°C for 24-36 h	Crushing and sieving (0.5-2.0 mm)	Exposure to chemicals (ZnCl$_2$) for 24 h, room temperature	Drying at 103°C for 24 h	Pyrolyzing under nitrogen flow (final temperature: 500°C)	Washing with HCL and water	Drying at 103°C for 24 h
(Khalili et al. 2000)	Raw material (sludge) dried at 110°C for 24 h	Crushing and sieving (smaller than 600 μm)	Exposure to chemicals (ZnCl$_2$) 85°C for 7 h	Drying at 110°C for 24–36 h	Crushing to fine powder and pyrolyzing under nitrogen flow, at 800°C for 2 h	Crushing	Drying
(Azargohar & Dalai 2008; Argyropoulos 2007)	Biochar material sieved and crushed (150-600 μm)	-	Exposure to (KOH) at room temperature for 2 h	Drying at 120°C overnight	Specified amount of sample placed in a fixed bed reactor was heated to 300°C for 1 h, before raising the temperature to the set point and held for 2 h	Washing with HCL and water until pH is between 6-7	Drying at 110°C for 12 h

According to (Azargohar & Dalai 2008), the chemical activation of pyrolyzed char via KOH is an effective process to increase the surface area and porosity. As mentioned before, the exact mechanism of the chemical activation is not well understood (Raymundo-Piñero et al. 2005; Argyropoulos 2007). However, in some literature the general reaction for chemical activation using potassium or sodium hydroxide is reported as follow Raymundo-Piñero et al. (2005):

$$6MOH + C \rightarrow 2M + 3H_2 + 2M_2CO_3 \tag{2.1}$$

In general, chemical activation by alkalis consists two main reactions of the hydroxide reduction and carbon oxidation to generate porosity (Raymundo-Piñero et al. 2005). CO, CO_2 and H_2 are evolved during the reaction and chemically activating agent is eliminated by washing with acid/base and water (Argyropoulos 2007).

2.4.2 Silica template method

The overall concept of template method is basically the same as fabricating a ceramic jar but narrowed down to the nano-meter scale (Lee et al. 2006). The first step to make a jar is to carve a piece of wood as a template with the desired shape followed by applying the clay on it. The second step is to heat up the clay at 1000°C under air so that the clay turns into ceramic while the wood burns simultaneously to create the empty space in the jar (as shown in Figure 2.6). One of the most commonly used templates to increase the porosity and surface area of carbon material is the mesoporous silica. Reported by Hu et al. (2006), in this method the carbon precursor (e.g., D-glucose) is dissolved into the pre-formed porous templates such as mesoporous silica and then carbonized at high temperatures. Finally the silica template is removed by washing with either NaOH or diluted HF solution to create a porous carbon network as shown in Figure 2.7. In the same study, Hu et al. (2006) proposed a new technique for silica template method using phosphoric acid in which the uniform pore size can be tuned up to 15 nm. The formation process includes the co-assembly of nano-composite network prepared from silicate and precursor (e.g., glucose) and a subsequent chemical activation via phosphoric acid. Phosphoric acid plays a bi-functional role in which it reacts with carbon precursor to produce phosphates and poly phosphates (i.e., removal

of these groups via carbonization will create porosity in carbon network) while it is also a chemical activation reagent by increasing the carbonization rate of precursor at lower temperatures. The detailed approach is provided in Section 3.2.1.
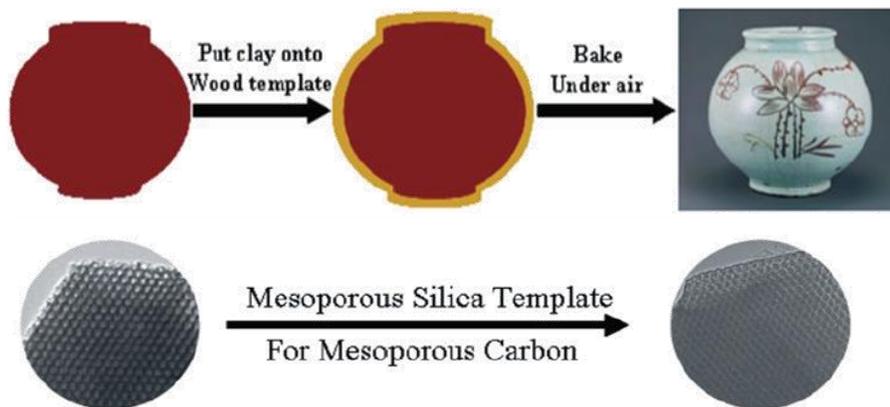
Figure 2.6. Schematic representation of the silica template concept (Lee et al. 2006)

In the mentioned method Tetra Ethyl Ortho-Silicate (TEOS) with the chemical formula of Si $(OC_2H_5)_4$ was used to form the silica template in addition of water, ethanol and hydrochloric acid as catalyst in a sol-gel process. TEOS is one of the ideal chemical precursors for sol-gel synthesis because it reacts readily with water (Sakka & Kamiya 1980). The hydrolysis reaction is one of the sol-gel synthesize reactions in which a hydroxyl ion becomes attached to the silicon atom in the TEOS molecule as follow (Dislich 1971):

$$Si\ (OR)_4 + H_2O\ \rightarrow HO\text{-}Si(OR)_3 + R\text{-}OH \tag{2.2}$$
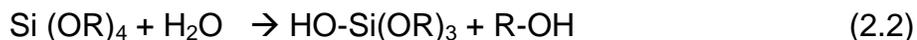
Hydrolysis reaction can be proceeded to completion based on the amount of water and catalyst present (i.e., HCL) so that all of the OR groups are replaced by OH groups. Any hydrolyzed molecule can attach to another one during a poly-condensation reaction (i.e., polymerization reaction in which small molecules such as alcohols and water is

released) to form the Si-O-Si linkages as shown in Equations (2.3) and (2.4). As the poly-condensation reaction proceeds the hydrolyzed TEOS molecules convert into a solid-like material with the Si-O-Si linkages (Dislich 1971; Yoldas 1979). Increasingly larger silicon-containing molecules can be continued to be generated by the process of polymerization.

$$(OR)_3–Si\text{-}OH + HO–Si\text{-}(OR)_3 \quad \rightarrow \quad [(OR)_3Si–O–Si(OR)_3] + H\text{-}O\text{-}H \qquad (2.3)$$

<div align="center">or</div>

$$(OR)_3–Si\text{-}OR + HO–Si\text{-}(OR)_3 \quad \rightarrow \quad [(OR)_3Si–O–Si(OR)_3] + R\text{-}OH \qquad (2.4)$$

(a)   **(b)**   **(C)**

Polycyclic Aromatic
Carbon Sheets
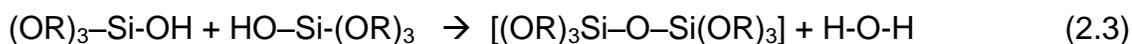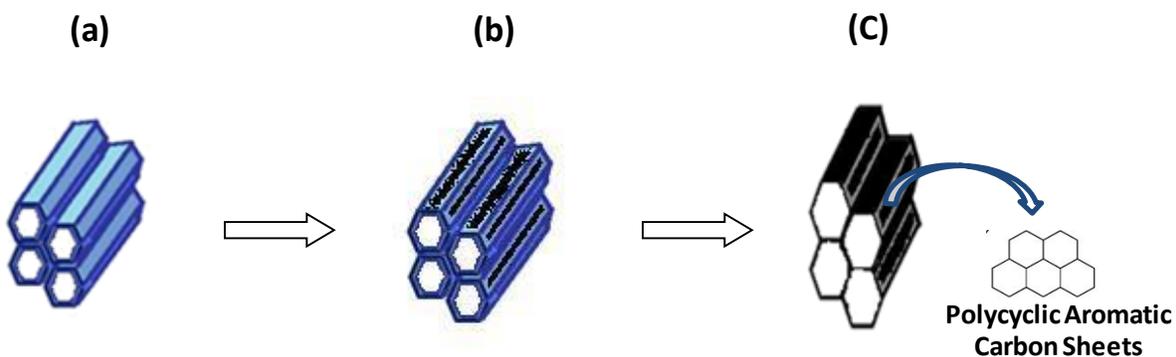
Figure 2.7. Preparation of porous carbon material via silica template method: (a) Synthesized silica template; (b) Silica template filled with D-glucose samples and carbonized at high temperature (i.e., 450°C); and Produced porous biochar support with removed silica template*

---

* Adopted from: Jidon Janaun. Development of sulfonated carbon catalyst for integrated biodiesel production. Chemical and Biological Departmental Seminar, University of British Columbia, October 29, 2009

2.4.3 Physical activation

The char obtained by carbonization of cellulosic materials is essentially microporous. This microporosity may become filled or partially blocked with tars and other decomposed products (Rodríguez-Reinoso & Molina-Sabio 1998). In order to enlarge the volume of micro-porosity, partial gasification of carbon material via CO_2, steam and air or a combination of them, can be performed. The main differences between gasification with carbon dioxide and steam are the larger dimension of CO_2 molecule compared with H_2O resulting in slower diffusion into the porous system of the carbon and restricted accessibility towards the micropores (Figueiredo et al. 1986). The basic reaction of carbon with water vapour is endothermic and of the following stochiometric form:

$$C + H_2O \rightarrow CO + H_2 \qquad\qquad (2.5)$$

Similarly, the reaction of carbon with carbon dioxide can be expressed as:

$$C + CO_2 \rightarrow 2CO \qquad\qquad (2.6)$$

In physical activation, the carbon atoms of the char network are oxidized by carbon dioxide or water molecules, thus, oxygen atoms are transferred and bonded to the carbon atoms. After decomposition of the oxygen surface groups, the resultant carbon monoxide molecules are desorbed from the network, generating porosity (Rodríguez-Reinoso & Molina-Sabio 1998). As the gasification reactions are endothermic, heat has

to be supplied in order to maintain an isothermal situation (Figueiredo et al. 1986). This gasification usually occurs at temperatures above 800°C (Figueiredo et al. 1986).

In some studies (Khalili et al. 2000; Hu et al. 2003) both chemical and physical activations of carbon material have been carried on as summarized in Table 2.4 (In most cases, chemical activation was performed prior to carbonization).

Table 2.4. Combined activation procedures for carbon-based material

Reference	1st step	2nd step	3rd step	4th step	5th step	6th step	7th step
	Chemical Activation					Physical Activation	
Hu et al. (2003)	Raw material (sludge) dried at 110°C for 24-36 h	Crushing and sieving (1-2 mm)	Exposure to chemicals ($ZnCl_2$ or KOH)	Drying at 110°C overnight	Pyrolyzing under nitrogen flow (final temperature: 800°C)	Gas flow in pyrolysis switch to CO_2 for 2 h	-
Khalili et al. (2000)	Raw material (sludge) dried at 110°C for 24 h	Crushing and sieving (smaller than 600 μm)	Exposure to chemicals ($ZnCl_2$) 85°C for 7 h	Drying at 110°C for 24–36 h	Crushing to fine powder & pyrolyzing under nitrogen flow at 800°C for 2 h	Crushing and drying the particles	Heating at 800°C for 2 h in a mixture of CO_2/CO

In the present study, the raw material used for the surface area and porosity development process is already in the form of pyrolyzed carbon, i.e., biochar, unlike similar studies in which the raw material are non pre-carbonized materials such as sludge, sugar, and wood. This might result in a slight change through the chemical mechanism of the process. However, recent studies (Argyropoulos 2007; Azargohar & Dalai 2008) show that physical and chemical activations of biochar through established

techniques are very effective, where the effects of temperature (600–900°C), mass ratio of steam to biochar (0.4–2), and activation time (0.9-4 h) on the porosity development in physical activation method have been studied. Similarly, the effect of activation temperature, mass ratio of KOH to biochar and nitrogen flow rate is investigated for chemical activation method via KOH treatment. In the physical activation method, by increasing the temperature, BET surface area is increased which is expected from an overall endothermic process such as steam activation (Raymundo-Piñero et al. 2005; Azargohar & Dalai 2008). Moreover, increasing the mass ratio of steam to char has the same effect since more oxidizing agent is available during the activation (Azargohar & Dalai 2008). In the chemical activation method, increasing the activation temperature and flow rate of nitrogen positively affect the amount of BET surface area. The effect of mass ratio of KOH/biochar has an optimum value of 1.93 while activation temperature and nitrogen flow were maintained at 800°C and 258 mL/min, respectively. Among all affecting parameters of the chemical activation method, the activation temperature has the highest impact (Azargohar & Dalai 2008). The maximum amount of BET surface area reported for chemically activated carbons is higher than that of physically activated carbons. Table 2.5 shows the range of variable parameters and consequent BET surface areas for chemical and physical activation approaches (Azargohar & Dalai 2008).

Table 2.5. Process parameters of physical & chemical activations for biochar according to Azargohar & Dalai (2008) and Argyropoulos (2007)

Activation Conditions	Chemical activation	Physical activation
Activation Temperature ($^\circ$C)	500-800	600-900
Mass ratio of oxidizing agent/Biochar	0.25-3	0.4-2
Nitrogen flow (mL/min)	80-250	-
Activation Time (h)	-	0.9-4
BET surface area range (m^2/g)	180-1500	300-950
Average pore diameter	13-15 A$^\circ$	13-26 A$^\circ$

3. Materials and Methods

3.1 Materials

Three biochar samples pyrolyzed from different sources of biomass were used: Sample 1, wood waste, white wood, bark and shavings; Sample 2, corn stover; and Sample 3, hardwoods and softwoods. All samples were as-received biochars and generated via fast pyrolysis process. Oleic Acid (NF/FCC), Methanol (99.9%, HPLC grade), Hydrochloric acid (A.C.S Reagent), Potassium Hydroxide (NF/FCC), Hydroflouric acid (48 wt.%) and Fuming Sulfuric acid (20% free SO_3) were obtained from Fisher Scientific while Tetraethyl Orthosilicate (TEOS), n-heptane, and standards used for GC analysis, i.e., methyl oleate and methyl linoleate, were obtained from Sigma-Aldrich. The canola oil (Canola Harvest) used for the transesterification was bought from a local grocery store.

3.2 Experimental Methods

3.2.1 Surface area and porosity development via silica template method

As mentioned in Section 2.4.2, the silica template method is one of the most commonly used techniques for surface area and porosity development of carbon material. In this method, the carbon material is introduced into the pre-formed porous template followed by carbonization and finally removal of the template (Hu et al. 2006). The preparation steps can be summarized as follow: (1) ~52 g of tetraethyl orthosilicate (TEOS) was mixed with acidic ethanol/water solution (the molar ratio of TEOS: water: ethanol: HCl was maintained at 1:6:6:0.1) and then kept in oven at 65°C for 4 hours; (2) ~22 g of biochar was then mixed with ~52 g of pre-reacted sol-gel, ~50 g of water, and ~10 g of

phosphoric acid (molar ratio of phosphoric acid to TEOS was 0.41) and then the mixture was stirred for 1 hour and dried at room temperature; (3) The resultant nano-composites were carbonized at 450°C in the tube furnace under nitrogen for 4 hours with the following temperature program: a ramp rate of 5°C/min from room temperature to 450°C, a dwell time of 4 hours followed by cooling to room temperature; and (4) Removal of silica template was conducted using 20% hydrofluoric acid for at least five times followed by washing with deionised water until no trace of acid is detected in the wash water (i.e., wash water pH turns neutral). The resultant activated biochar material was then dried in oven at 110°C overnight.

3.2.2 Surface area and porosity development via chemical activation method

Another technique utilized for surface area and porosity development of biochar samples was the chemical activation method with KOH as the activating reagent. ~24 g of biochar was ground, sieved (between the 38 and 250 μm mesh sizes) and then mixed with 150 mL of 7 mol/L KOH solution and stirred for 2 hours at room temperature to ensure the access of activating reagent to biochar samples (Azargohar & Dalai 2008). After filtration, the resultant carbon material was dried in oven at 110°C. Dried biochar samples were then carbonized at three different temperatures – 450, 675, and 875°C – under nitrogen flow (258 mL/min). The obtained samples were washed with deionized water followed by treatment with 250 mL of 0.1 mol/L HCl solution (Azargohar & Dalai 2008). Another washing step with deionized water was conducted in order to remove the HCl and the resultant activated biochar samples were dried in oven at 110°C overnight. The detailed process steps are depicted in Figure A.1 in Appendix.

3.2.3 Catalyst functionalization

The biochar samples (ground and sieved between the +38 and -250 μm mesh sizes) were mixed with fuming sulphuric acid (20% free SO_3) as functionalizing reagent. The mass ratio of Acid/Biochar was 16.5/1 and sulfonation time set to 15 hours under nitrogen flow (50 mL/min) at 150°C in accordance with the literature (Toda et al. 2005; Okamura et al. 2006; Zong et al. 2007; Mo et al. 2008a). The resultant samples were washed with hot distilled water at least for seven times until the pH of the wash water became neutral. The sulfonated biochar sample was then dried in oven at 110°C overnight.

3.2.4 Transesterification reaction

Transesterification of canola oil with methanol as alcohol reagent was done in a 25 mL batch reactor in an oil bath at 65°C under reflux. The powder catalyst was pre-dried in the oven at 110°C for about two hours prior to reaction. Methanol and pre-dried catalyst were mixed and stirred for 15 minutes and canola oil -which was preheated to reaction temperature (65°C) was slowly added to the mixture of methanol and catalyst. The reaction time was set to 24 hours and samples were collected at the end of reaction. Three samples were collected from product mixture each time in order to check the homogeneity of samples. The obtained samples were then diluted with n-heptane as solvent to prepare it for Gas Chromatography (GC) for analyses. The reaction conditions were maintained as follows: 15:1 Alcohol to Oil molar ratio, 5 wt.% catalyst loading based on the weight of canola oil, and a reaction temperature of 65°C.

Transesterification runs at high temperature/pressure conditions are conducted in a mini Autoclave reactor outfitted with a 100 mL vessel (MAWP[1]: 20 MPa at 315°C, Autoclave Engineers Co). A CT1000 control tower is used to control the reaction parameters such as temperature, pressure, and agitation rate. Nitrogen was used as the inert gas in the reactor while methanol and canola oil were utilized as alcohol reagent and fresh vegetable oil feedstock, respectively. Reaction conditions such as the alcohol to oil molar ratio and catalyst loading were set to 15:1 and 5 wt.%, respectively, similar to the transesterification runs performed under atmospheric conditions. The reaction time has been decreased to 3 and 6 hours while the reaction temperature has been increased to 150°C under 1.52 MPa (gauge) pressure in order to prevent the evaporation of methanol at high temperature. The same aforementioned method of product analysis is utilized to quantify the amount of produced methyl esters.

3.2.5 Esterification reaction

Esterification reaction was conducted in the presence of oleic acid, as a model compound for long chain fatty acid, and methanol as alcohol reagent. Similar to transesterification reaction, a 25 mL batch reactor in an oil-bath at 65°C was used under reflux condition. The catalyst was pre-dried prior to the reaction and mixed with methanol exactly in the same way as mentioned earlier for transesterification reaction. 18:1 alcohol to oil molar ratio, 10 hours reaction time, and 5 wt.% catalyst loading were applied as reaction conditions. Since the esterification products (i.e., water and methyl oleate) were immiscible, the product samples were extracted while simultaneously stirring the solution. Three different samples were obtained each time to check the

---

[1] Maximum Allowable Working Pressure

homogeneity of the products, and the reproducibility of the results. The obtained samples were then diluted with n-heptane and centrifuged at 10,000 rpm for 10 minutes. The upper layer was taken and diluted again with n-heptane for GC analysis.

3.2.6 Transesterification yield

In this study yield has been defined as the mass ratio of produced methyl esters over the oil used as substrate (Shimada et al. 1999; Supple et al. 2002). To calculate the yield, the volume of products was calculated from the mass and density of the product mixture upon completion of the reaction. The catalyst mixed with the products was separated using a centrifuge at 10,000 rpm for 20 minutes upon completion of the reaction. Density of the separated products was measured using a micro pipette. By dividing the mass by the density of products, the volume was calculated. Furthermore, the concentrations of methyl esters (mostly methyl oleate and methyl linoleate since canola oil is mainly compromised of C:18 fatty acids) in the product mixture were obtained from the GC analysis. By calculating the volume of products and the concentrations of each methyl ester, the total mass of methyl ester present in the product mixture has been calculated. The yield was then obtained by dividing the mass of produced methyl esters by the mass of initial canola oil used as substrate.

3.2.7 Esterification conversion

To quantify the esterification conversion, the acid number values of the oil phase before and after reaction were calculated. The following equation was used to calculate the conversion (Sejidov et al. 2005):

$$Conversion\ (\%) = \left[\frac{(a_1 - a_2)}{a_1}\right] \times 100 \qquad (3.1)$$

Where a_1 and a_2 are acid number values (mg KOH/g Oil) of oil before and after esterification, respectively. Product mixtures upon completion of the reaction were centrifuged to allow phase separation. Then the oil phase was recovered and titrated for acid number value according to the ASTM D664 using Metrohm 794 autotitrator.

3.3   Characterization Methods

3.3.1 Gas chromatography (GC) analysis

The GC technique involves the separation of the different compounds in a mixture based on their partitioning between a stationary liquid phase and a moving gas phase (i.e., Helium). Each component has a specific "retention time" on the column before passing to the detector. The signal intensity from the detector is proportional to the concentration of the components, including the methyl esters in this study. Hewlett Packard (HP) dual 5890 with a flame ionization detector and DB5 capillary column was used for GC analysis. After separation of catalyst from the product mixture, the products were diluted with n-heptane as solvent to be ready for GC analysis. Three different diluted solutions of the reaction products have been prepared from three different parts of the product batch in order to check the reproducibility. Calibration curves were obtained each time prior to product analysis using methyl oleate and methyl linoleate pure GC grade standards (Sigma-Aldrich). GC analyses have been conducted in the Biofuel Laboratory in the Department of Chemical & Biological Engineering at the University of British Columbia (UBC), Canada.

3.3.2 Total acid density and sulfonic group density

The total acid density of catalyst samples was determined using the standard acid-base back titration method on a 794 Basic Titrino (Metrohm AG) auto-titrator. The catalyst samples were pre-dried in the oven at 110°C for at least two hours prior to analysis, then ~0.10 g of catalyst was added into 60 mL of 0.0080 mol/L NaOH and stirred for 30 minutes before back-titration with 0.02 mol/L HCl. Three different acidic groups of sulfonic, carboxylic and phenolic constitute the total acid density. As reported by (Mo et al. 2008a), sulfonic group contributes much to transesterification reaction compared to the other two acidic groups, i.e., carboxyl and phenolic. These two groups are the result of oxidization of aliphatic groups due to strong sulfonation and incomplete carbonization of the supporting material. In order to measure the sulfonic group density of each catalyst as well as the total acid density, the catalyst samples were sent for elemental analysis (Section 3.3.3). According to literature (Okamura et al. 2006; Takagaki et al. 2006; Nakajima et al. 2007; Zong et al. 2007; Mo et al. 2008a), it is assumed that all sulfur content of each sample is in the form of $-SO_3H$, i.e., sulfonic group. Thus, the sulfonic group density can be calculated based on the weight percentage of S content over the total of other constituent elements (i.e., Oxygen, Hydrogen, Carbon, and Nitrogen). The higher estimated values of total acid density comparing to sulfonic group density can be explained by the presence of two other acidic groups, i.e., carboxylic and phenolic, in the total acid density values as explained above. Total acid density analyses have been conducted in the Biofuel Laboratory in the Department of Chemical & Biological Engineering at the University of British Columbia.

3.3.3 Elemental analysis

The carbon, hydrogen, nitrogen, sulfur and oxygen content of the biochar-based catalysts were determined via Elemental Analysis conducted by Canadian Microanalytical Service Ltd., Delta, British Columbia.

3.3.4 Surface area and porosity

The Brunauer-Emmet-Teller (BET) method is the most widely used method for calculating the total surface area (Gregg & Sing 1982). The surface area of each sample was measured based on BET multipoint method using Micromeritics ASAP 2020. Nitrogen was used as the adsorbate gas to construct adsorption/desorption isotherms for the porous carbon samples using liquid nitrogen at 77K to keep the temperature constant. The quantities of adsorbed and desorbed nitrogen on and from the samples at different relative pressures (i.e., P/P_0 points where P is the gas pressure and P_0 is the saturation pressure of adsorbate gas) were measured by the ASAP 2020 equipment.

Both of micropore and mesopore volumes have been calculated using Micromeritics ASAP 2020 based on t-plot and Barrett, Joyner and Halenda (BJH) methods, respectively (Gregg & Sing 1982; Webb & Orr 1997). The total pore volume is calculated based on the sum of micropore and mesopore volumes (Gregg & Sing 1982; Hu et al. 2001). Prior to each surface area and porosity measurement, ~ 0.6 g of each sample was degassed for approximately 5 hours in order to eliminate any adsorbed species on the surface. The degas step was based on the Silica-Alumina procedure and included two phases: evacuation and heating. Evacuations have been conducted at 5 mm Hg/min to the total pressure of 10 μm Hg followed by holding pressure at 10 μm Hg

for two hours. Heating phase included the heat ramp of 10°C/min to the set-point of 120°C followed by a 120-minute dwell time. The surface area and porosity analyses have been conducted in the Analytical Laboratory in the Department of Chemical & Biological Engineering at the University of British Columbia.

3.3.5 Fourier transform infrared (FT-IR) spectroscopy

The presence of functional groups on the surface of each catalyst sample was analyzed using Fourier Transform Infra Red spectroscopy (FT-IR) with the ATR (attenuated total reflectance) technique instead of the more conventional KBr technique usually utilized in the analysis of carbon-rich samples such as chars and coals mainly due to the ease of operational steps of the analysis since ATR requires very little or no sample preparations. Moreover, ATR is suitable for analyzing solids, especially dark-colored materials with strong IR absorption. FT-IR analysis was performed using a Varian 3100 FT-IR Excalibur Series spectrometer fitted with a Pike MIRacle™ATR sampling accessory and running Resolution Pro software. Spectra were collected at a resolution of 4 cm^{-1}, an aperture setting of 4 cm^{-1}, a scan speed of 1.2 kHz over a wavenumber range of 4000-650 cm^{-1}. The ATR was equipped with a ZnSe crystal and 64 scans were co-added for each sample to enhance the signal-to-noise ratio.

3.3.6 X-ray diffraction (XRD) spectroscopy

This analysis is one of the most commonly used techniques for crystalline phase identification. In this technique, the catalyst sample is irradiated with X-ray of a known wavelength (λ). Consequently, X-rays are reflected by atomic layers with interplanar spacing (d) at the certain angle of incidence and reflection known as Bragg angle (θ) (Reed 2005). Powder XRD patterns of the prepared catalysts were analyzed on a

Bruker AXS D8 Advance X-ray Diffractiometer (in Bragg-Brentano configuration) equipped with a NaI scintillation detector and diffracted beam graphite monochromator. Cu Kα1,2 radiation was generated at 40 kV and 40 mA and recorded over the range of 2θ from 5 to 60°C. A custom-made sample holder with a shallow well was used for the samples, and rotated to improve particle statistics. These analyses have been performed in the X-Ray Laboratory in Department of Chemistry at the University of British Columbia.

4.   Results and Discussions

4.1 Surface Area and Porosity Development of Biochar

Generally biochar has significantly low surface area and porosity. In this study two different activation methods have been conducted to increase the surface area and porosity (e.g., pore size and pore volume) of biochar: silica template method (Hu et al. 2006); and KOH chemical activation method (Azargohar & Dalai 2008). As shown in Table 4.1, the former method resulted in a significant increase in BET surface area of the biochar sample. However, compared to the chemical activation method with KOH, increase in surface area obtained via the silica template method was much lower (116 vs. 204 m^2/g) while requiring more complicated and time consuming preparation steps. Thus, further investigations have focused on the chemical activation method with KOH. This method was applied on Biochar Sample 1 (i.e., pyrolyzed from wood waste, barks and shavings) at three different temperatures (450, 675, and 875°C), and also on Biochar Samples 2 and 3 (i.e., pyrolyzed from corn stover and softwoods/hardwoods respectively) at 675°C for further comparisons. As shown in Table 4.1, increasing the activation temperature from 450 to 875°C of Biochar Sample 1, the surface area and the total pore volume had increased considerably.

Biochar-based catalysts supported on activated biochar material via chemical activation method were prepared and compared. As mentioned earlier, catalyst preparation was done through sulfonation process in the presence of fuming sulphuric acid. As it is shown in Table 4.1, the BET surface area and the total pore volume of the activated supports were reduced after sulfonation (especially in the case of activated support at 450°C). The surface area reduction can be attributed to the dissociation of sp^3-based

carbon bonds (C-C linkage) between carbon sheets due to the harsh sulfonation (Ertl et al. 1999; Okamura et al. 2006; Xing et al. 2007). By increasing the activation temperature the number of C-C bonds in the carbon lattice increases, hence the degree to which the pores collapse, has decreased as clearly shown in Table 4.1 (% decrease in surface area after sulfonation).

Table 4.1. Surface area and porosity of activated biochar samples before and after sulfonation

Activation Method- Activation Temperature (°C)	Biochar Sample	BET surface area (m^2/g)		Pore size (nm)		Total Pore Volume[1] (cm^3/g)		% Decrease in surface area after sulfonation
		Before sulfonation	After sulfonation	Before sulfonation	After sulfonation	Before Sulfonation	After sulfonation	
Without activation	1	<0.5	-	N.Q.[2]	-	N.Q.	-	-
STM[3]- 450	1	116	-	1.97	-	0.046	-	-
CAM[4]-450	1	204	1.58	2.62	N.Q.	0.12	0.01	99%
CAM[3]-675	1	668	640	2.22	2.17	0.37	0.35	4%
CAM[3]-875	1	1469	1410	2.24	2.20	0.77	0.71	4%
CAM[3]-675	2	726	676	2.09	2.05	0.36	0.36	7%
CAM[3]-675	3	776	783	1.91	1.91	0.37	0.34	-

---

[1] Total pore volume= t-plot micropore volume+ BJH Desorption mesoporous volume
[2] Not Quantifiable due to the instrument limitations for low BET surface area
[3] Silica Template Method, for reaction conditions and steps refer to Section 3.2.1
[4] Chemical Activation method with KOH, for reaction conditions and steps refer to Section 3.2.2

4.2 Transesterification Activity

4.2.1 Effect of stronger functionalizing

A preliminary study on sulfonated biochar-based catalysts indicated considerable esterification activity in FFAs conversion (~ 90%) to biodiesel from waste vegetable oil feedstock (West 2006). However, the prepared catalyst showed very poor activity for transesterification of triglyceride-based oils such as canola oil. Thus, further investigation was conducted to improve the catalytic activity of the transesterification of triglyrecides. The first step in developing the biochar-based catalyst was to perform a stronger functionalizing process by changing two parameters based on West's study (2006): sulfonation reagent (fuming sulphuric acid vs. concentrated sulphuric acid) and Acid/Char ratio (16.5:1 vs. 10:1). As a result of these changes, the total acid density of the biochar catalyst increased by almost 90 times (0.036 vs. 2.6 mmol/g) resulting in considerable increased transesterification yield from being negligible to ~9% (Table 4.2). Aside from the two mentioned changes, the rest of the sulfonation conditions (e.g., temperature, time, nitrogen flow) were identical to West's study (Section 3.2.3).

Table 4.2. Different sulfonation processes and corresponding transesterification yields

Sulfonation Reagent	Acid/ Char ratio	Total Acid Density (mmol/g)	Transesterification Yield
Concentrated sulphuric acid (98%)[1]	10 : 1	0.036	Negligible
Fuming sulphuric acid (20% free SO_3)	16.5 : 1	3.2	8.6 ± 0.6[2]

---

[1] (West 2006)

[2] As mentioned in Sections 3.2.4 and 3.3.1, the average values and standard deviations have been calculated based on the results of three different samples from product mixture of one reaction. The reaction was not repeated.

4.2.2 Combined effects of support treatment and different sulfonation times[1]

According to the literature, increasing the surface area and pore structure of the catalyst (e.g., pore size and pore volume) improves the intra-particle diffusion of reactants resulting in higher transesterification yield (Suppes et al. 2004; Kulkarni et al. 2006). However, it has also been reported that the effect of surface area on the activity of carbon-based catalysts for biodiesel production is less than that of the total acid density and sulfonic group density (Mo et al. 2008b). In order to study the effect of surface area and porosity development on transesterification activity, the combined effect of treating the biochar support and the sulfonation times (5 and 15 hours) on methyl ester production were investigated. The biochar support was treated using a chemical activation method with 7 mol/L KOH at 450°C with a specific KOH to biochar mass ratio under nitrogen flow (see Section 3.2.2 for the detailed process). The treated and untreated biochar supports then underwent sulfonation for either 5 or 15 hours following the sulfonation process described in Section 3.2.3. The resulting biochar-based catalysts were then washed with distilled water and filtered. The washing/filtration process has been done continuously with hot distilled water (>80°C) for several times until no sulfate ions could be detected in the wash water upon determination of the pH. The resulting slurry was dried in the oven at 110°C overnight. The four resultant catalysts (nomenclature shown in Table 4.3) have been studied for their catalytic activity in the transesterification of canola oil with methanol using similar reaction conditions as

---

mentioned in Section 3.2.4. The prepared catalysts were characterized by elemental analysis, total acid density, and BET surface area analysis.

Table 4.3. Identification of four different catalysts prepared

Catalyst Samples	Support treatment	Sulfonation Time (h)
Cat (-,-)	No	5
Cat (+,-)	Yes	5
Cat (+,+)	Yes	15
Cat (-,+)	No	15

The total acid density of the four resultant catalysts was measured via back titration method as explained in Section 3.4. As mentioned earlier, the total acid density consists of three different acidic groups; sulfonic, carboxylic, and phenolic. The density of sulfonic group was also calculated via elemental analysis results. According to the literature (Okamura et al. 2006; Takagaki et al. 2006; Nakajima et al. 2007; Zong et al. 2007; Mo et al. 2008a), it is assumed that all sulphur content of each sample is in the form of $-SO_3H$. The difference between the amount of total acid density and sulfonic density can be explained by the presence of phenolic and carboxylic groups in addition to sulfonic groups in the total acid density values. As shown in Table 4.4, similar to the total acid density values, the sulfonic group densities of all catalyst samples are slightly different.

The surface area of the prepared catalysts was measured using ASAP 2020 instrument (Section 3.2.1). Surface area development on the original biochar increased the surface area from <0.5 to 204 m^2/g. However, as indicated in Table 4.4, the developed surface area has collapsed and decreased drastically after sulfonation, as also noted by Peng et

al. (2010). Dissociation of the C-C linkage between carbon sheets due to the harsh sulfonation is a possible reason for this significant reduction in (Section 4.1). Furthermore, the surface area of the catalyst supported on untreated biochar, Cat (-,+), is greater than the surface area of the catalyst with treated biochar, Cat (+,+), when prepared under the same sulfonation conditions. This could be explained by the higher fines content in the former catalyst as compared to the latter one, while each catalyst had the same particle size of less than 250 and over 38 μm. Thus, it can be concluded that the effect of surface area development is eliminated by the significant collapse of the structure of treated support after sulfonation.

Table 4.4. Characterization results of prepared catalyst for studying combined effects of sulfonation time and surface area development

Sample	Total Acid Density (mmol/g)	Sulfonic Group Density[1] (mmol/g)	BET Surface Area (m^2/g)	Particle Size Range (μm)
Untreated Biochar	-	-	<0.5	-500, +180
Treated Biochar	-	-	204	-500, +180
Cat (-,+)	3.2	0.961	2.46 ± 0.04	-250, +38
Cat (+,+)	2.6 ± 0.1	0.839	1.58 ± 0.05	-250, +38
Cat (+,-)	2.5 ± 0.1	0.911	1.40 ± 0.10	-250, +38
Cat (-,-)	2.8 ± 0.1	0.995	0.69 ± 0.02	-250, +38

The concentration of methyl esters produced through the transesterification of canola oil was measured via gas chromatography method as explained in Section 3.3.1. Only the

---

[1] Calculated based on Elemental Analysis

concentration of Methyl Oleate (MO) and Methyl Lin-Oleate (MLO) were monitored since canola oil is mainly consists of C:18 fatty acids, i.e., oleic and Linoleic acids. The catalyst with the highest surface area and acid density, Cat (-,+), showed the highest catalytic activity for the production of methyl esters from canola oil. Comparison of the methyl ester conversion for Cat (+,+) vs. Cat (+,-) in Figure 4.1 indicates an increasing conversion with increasing surface area for a similar total acid density. Thus, surface area and porosity of the carbon-based catalyst is another influential factor on catalytic activity in addition to the total acid density or sulfonic group density. Further investigations on surface area and porosity development (i.e., pore size and pore volume) were performed in the following section.
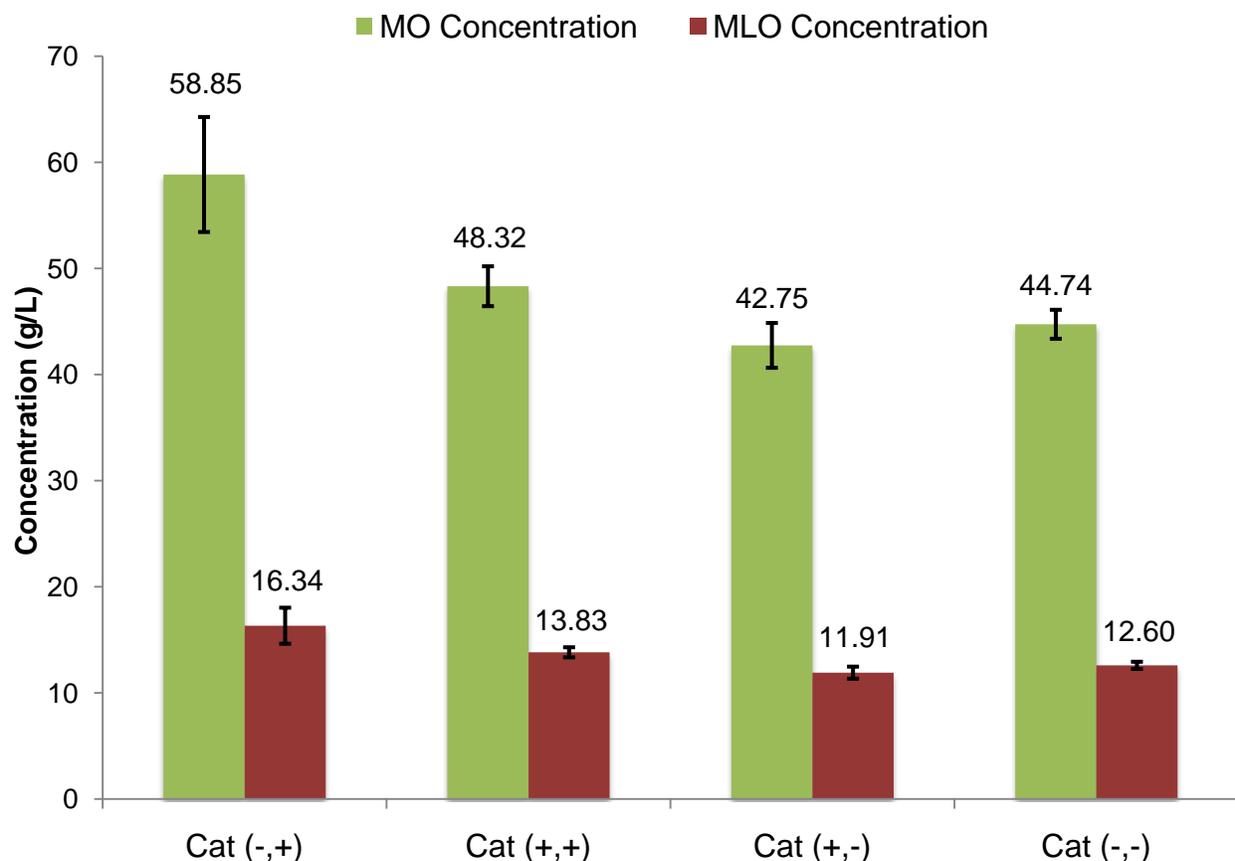
Figure 4.1. Produced amounts of MO and MLO[1] versus different types of catalysts

4.2.3 Effect of surface area and porosity development [2]

Three catalysts with activated supports (Biochar Sample 1) at three different temperatures- 450, 675, and 875°C- have been studied for their transesterification activity using methanol. All of the biochar supports have been activated via chemical activation method with KOH. As discussed in Section 4.1, the higher the activation temperature, the higher the surface area of the activated support. Furthermore, the

---

[1] As mentioned in Sections 3.2.4 and 3.3.1, the average values and standard deviations have been calculated based on the results of three different samples from product mixture of one reaction. The reaction was not repeated.

[2] Another version of this section is ready to be submitted to journal of *Fuels & Energy*

activated support at the lowest activation temperature (i.e., 450°C) showed a considerable reduction in the surface area and pore volume after sulfonation. Nevertheless, the percentage of the surface area reduction was reduced considerably (99% vs. 4% reduction) for the sulfonated supports activated at higher temperatures, i.e., 675 and 875℃, as shown in Table 4.1. This might be explained by the structural changes of the activated supports due to the higher activation temperatures. The total acid density of each catalyst was measured via back titration method (Section 3.3.2). Since the total pore volume increased with increasing activation temperature, it was expected that the total acid density of the catalyst samples would increase, as the increase in the pore size would allow the sulfonic groups to be more easily incorporated onto the carbon matrix. However, increasing the activation temperature led to an unexpected decrease in the total acid density and consequently sulfonic group density, as shown in Table 4.5. This decrease can be attributed to the lesser amount of polycyclic aromatic carbon available to be functionalized in the activated supports at higher temperatures, i.e., 675 and 875°C, mainly due to the more ordered structure in align with Xing et al. (2007). Further discussion is included in Section 4.5.

Table 4.5. Physical characteristics of catalysts with activated supports (Biochar Sample 1) at different temperatures

Activation temperature (°C)	Total Acid Density (mmol/g)	Sulfonic group Density (mmol/g)	Surface Area (m^2/g)	Total Pore Volume[1] (cm^3/g)	Transesterification Yield (%)
450	2.6 ± 0.1	0.839	1.58	0.01	7.6 ± 0.6
675	1.2 ± 0.1	0.405	640	0.35	18.9 ± 0.6
875	0.43	0.377	1410	0.71	8.4 ± 0.3

---

[1] Total Pore Volume= t-plot micropore volume + BJH Desorption mesopore volume

All prepared catalysts were tested for transesterification activity with the same reaction conditions reported in Section 3.2.4. As shown in Table 4.5, increasing the activation temperature from 450 to 675°C resulted in increasing the transesterification yield to almost twice of its value. This may be due to the significantly higher surface area and pore volume of the catalyst with activated support at 675°C despite of the lower total acid density value. However, when the activation temperature was further increased to 875°C, instead of the expected increase in catalytic performance, the yield dropped back to about the same as that obtained for 450°C. This amount of reduction in the transesterification yield can be explained by the significant reduction of the total acid density and sulfonic group density in spite of increased surface area and porosity while increasing the activation temperature of the biochar support. These results suggest that the catalytic activity of the biochar is dependent on both surface area as well as total acid density and that the maximum would be obtained from an activation temperature, most probably between 675 and 875°C. So far, the best biochar-based catalyst that yielded the highest transesterification activity is the one with activated support at 675°C. The mentioned catalyst was further investigated for the esterification of free fatty acids such as oleic acid in the presence of methanol in Section 4.3.

4.3 Esterification Activity

According to the results of catalytic activity in transesterification reaction, the catalyst supported on the activated biochar (Sample 1) at 675°C resulted in the highest yield. In order to test the activity of this catalyst for esterification of FFAs as well as transesterification of TGs, esterification of oleic acid in the presence of methanol was tested for the mentioned catalyst. The reaction conditions were explained in Section

3.2.5. Upon completion of the reaction, the oil phase was separated and tested for acid number value. The reaction conversion was calculated based on the acid number value of oil phase before and after reaction. Three samples from product mixture have been obtained after completion of the reaction to test the reproducibility of results. The esterification conversion was 97.1 ± 2.8%.

4.4 Biochar-Based Catalysts Supported on Different Biochar Samples

Thus far, it has been shown that the as-received biochar sample pyrolyzed from a mixture of wood wastes, white wood, bark and shavings (i.e., Biochar Sample 1) can be utilized for biodiesel production from both transesterification of canola oil and esterification of oleic acid using methanol. The best activation conditions yielded the most active biochar-based catalyst, i.e., with chemically activated support via KOH at 675°C, was applied to two other biochar samples produced from different feedstocks; one from corn stover, i.e., Biochar Sample 2 and the other one from softwoods and hardwoods, i.e., Biochar Sample 3. Table 4.6 shows the comparison of physical characteristics (e.g., total acid density, surface area, and pore volume) of the three aforementioned catalysts prepared from biochar samples 1, 2, and 3 with activated supports at the same temperature (675°C). More detailed BET surface area and pore volume results of the mentioned activated biochar samples (after and before sulfonation) were previously presented in Table 4.1.

Table 4.6. Characterization of three different catalysts supported on activated biochars from different feedstocks

Biochar Sample	Activation Temperature (°C)	Surface Area (m^2/g)	Total Pore Volume (cm^3/g)	Total Acid Density (mmol/g)
1	675	640	0.35	1.2 ± 0.1
2	675	726	0.34	1.3 ± 0.1
3	675	776	0.36	1.4 ± 0.1

Transesterification activities of three produced catalysts were compared and showed in Table 4.6. Reaction conditions such as alcohol to oil molar ratio (15:1), catalyst loading (5 wt.%), reaction temperature (65°C) under atmospheric pressure were similar to what has been explained in Section 3.2.4 for atmospheric runs. Surprisingly, catalysts supported on activated Biochar Samples 2 and 3 showed significantly low transesterification yields, i.e., less than 1%, comparing to biochar-based catalyst from Sample 1. Since the total acid density and the total pore volume of all catalysts are very similar, one possible reason for the significant difference of transesterification yields can be attributed to the higher pore volumes of larger pores in the catalyst supported on Biochar Sample 1 as evidenced by Pore Size Distribution (PSD) shown in Figure 4.3. However, it is worth noting that different pyrolysis parameters such as process temperature and reaction time can affect the structure of the produced biochar and consequently catalyst supported on produced biochar (Brewer et al. 2009). More importantly, biochar can be far more complex when it has been prepared from different feedstocks since its composition depends largely on the biomass feedstock. Depending on the feedstock, not all chars are suitable for combustion or activation applications; for

example, those containing higher levels of silica ash such as those from switchgrass and corn stover are generally more suitable for soil applications (Brewer et al. 2009). Thus, further understanding of the effects of pyrolysis process and the origin of the feedstocks on catalytic activity is warranted.
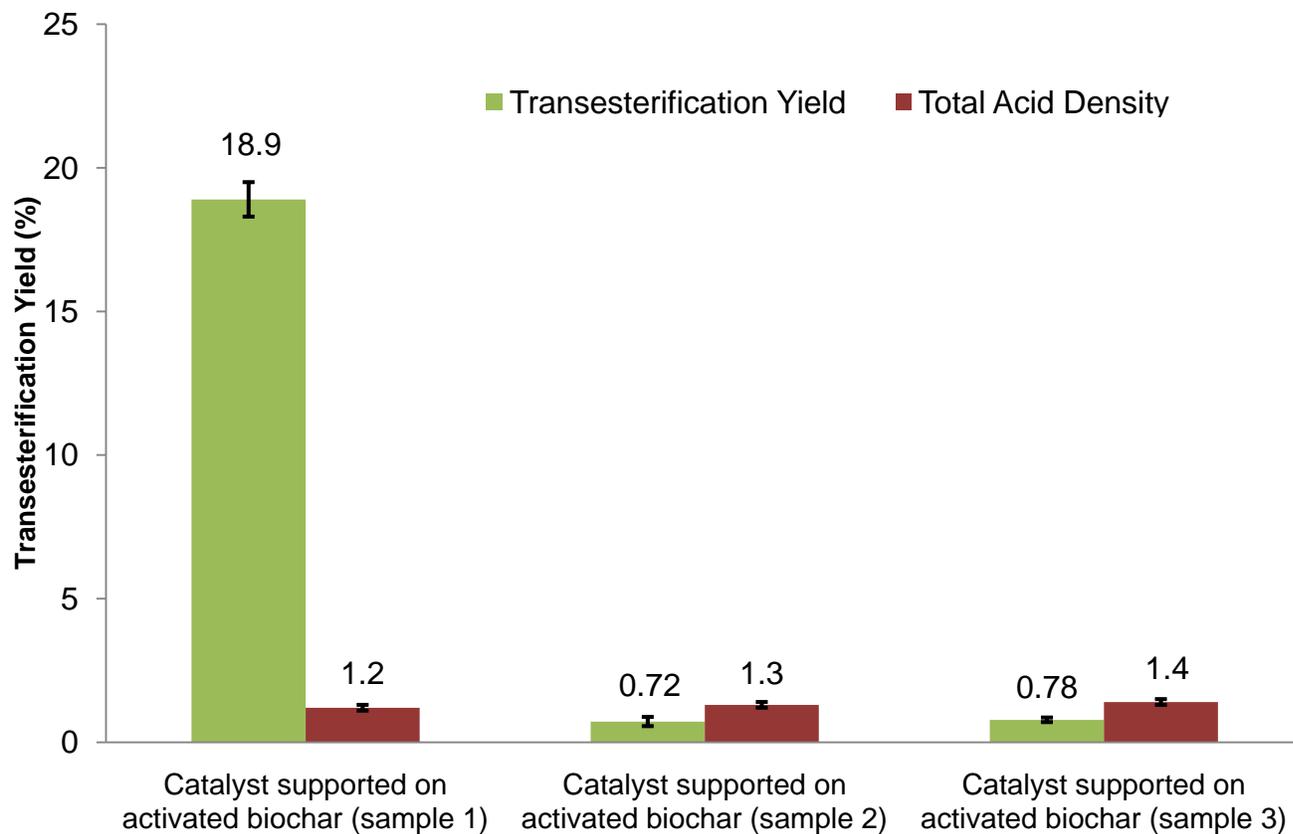
Figure 4.2. Transesterification yields and total acid densities of three catalysts supported on different activated biochar samples
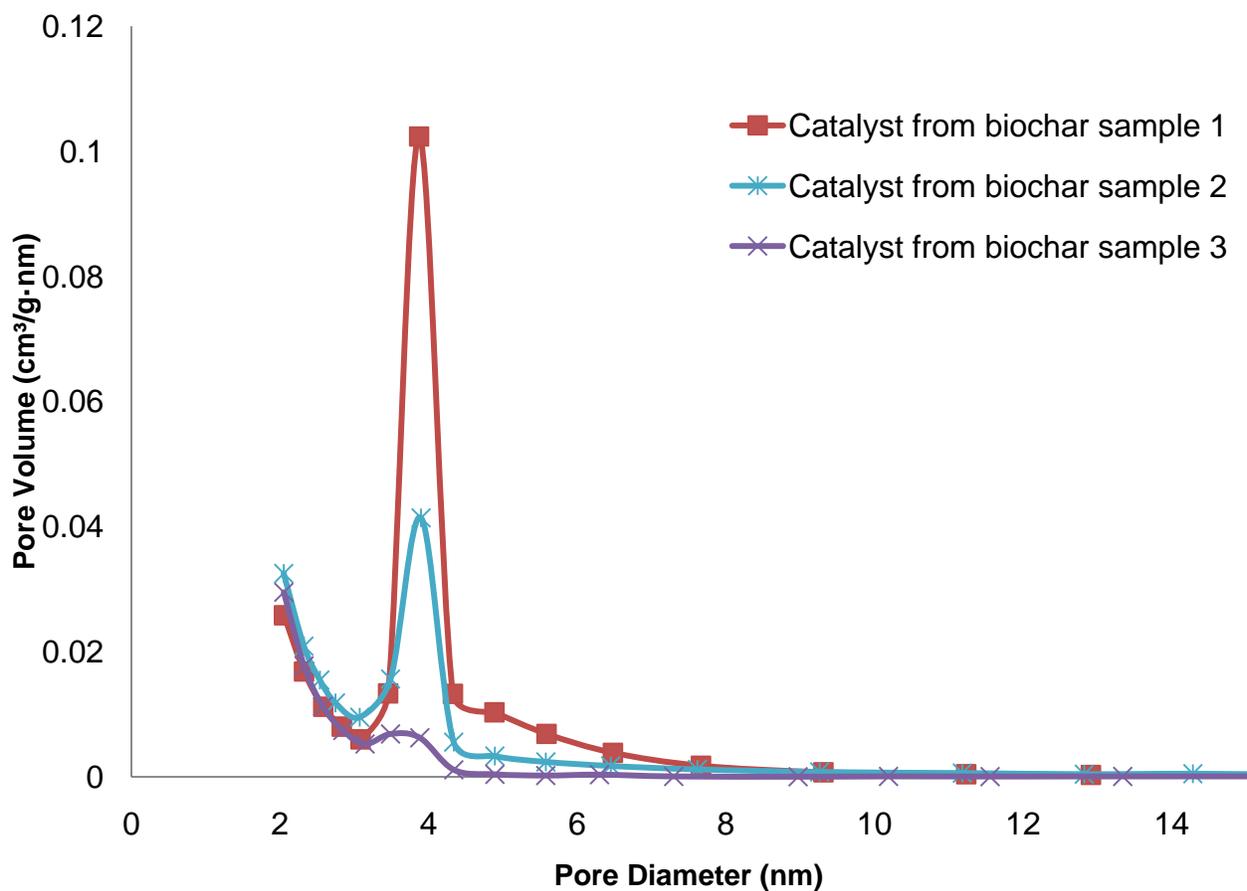
Figure 4.3. Pore Size Distribution (PSD) of prepared biochar-based catalysts from different biochar samples

4.4.1 Effect of higher temperature/pressure conditions

According to Nakajima et al. (2007) and Melero et al. (2010), conducting transesterification of triglyceride-based oils with methanol under high temperature/pressure conditions results in high methyl ester yields. In order to investigate the effect of high temperature/pressure on the transesterification reaction two preliminary runs have been conducted in a mini Autoclave reactor. The reaction temperature was 150°C and the pressure was 1.52 MPa (gauge pressure) in order to

prevent the evaporation of methanol. Reaction time was set to 3 and 6 hours while the alcohol to oil molar ratio and catalyst loading were maintained as 15:1 and 5 wt.%, respectively.

Two catalyst reagents were tested: the catalyst with activated biochar (Sample 3) at 675°C which was one of the lowest yielded catalysts; and, the best catalyst based on the atmospheric transesterification runs, i.e., the one with activated biochar (Sample 1) at 675°C. As shown in Table 4.7, conducting the transesterification under high temperature/pressure conditions using the former catalyst resulted in considerable increase in the concentration of produced MO and MLO.

Table 4.7. Methyl ester production via transesterification under high temperature/pressure vs. atmospheric condition for catalyst supported on Biochar Sample 3

Catalyst Sample	Reaction Conditions[1] (Temperature/Pressure, Time)	MO concentration[2] (g/L)	MLO concentration (g/L)
Supported on activated biochar (Sample 3) at 675°C	150°C/1.52 MPa, 3 h	156.10 ± 13.43	59.88 ± 5.02
	150°C/1.52 MPa, 6 h	61.51 ± 3.18	14.86 ± 0.76
	65°C/atmospheric, 24 h	3.97 ± 0.36	0.82 ± 0.37

Moreover, using the latter catalyst, i.e., the best catalyst based on the atmospheric transesterification runs, resulted in higher reaction yield but in a significantly lower reaction time comparing to atmospheric runs (3 vs. 24 hour), as shown in Table 4.8.

---

[1] All reaction conditions except for temperature/pressure and time were maintained constant, i.e., alcohol to oil molar ratio 15:1 and catalyst loading 5 wt.% based on canola oil.
[2] As mentioned in Sections 3.2.4 and 3.3.1, the average values and standard deviations have been calculated based on the results of three different samples from product mixture of one reaction. The reaction was not repeated.

Table 4.8. Effect of high temperature/pressure condition on transesterification yield of catalyst supported on Biochar Sample 1

Catalyst Sample	Reaction Conditions	Reaction Yield [1](%)
Supported on activated biochar (Sample 1) at 675°C	150°C/1.52 MPa, 3 h	24.5 ± 0.5
	65°C/atmospheric, 24 h	18.9 ± 0.6

4.4.2. Reaction time and transesterification yield in high temperature/pressure runs

Conducting transesterification runs under high temperature/pressure condition resulted in higher MO and MLO concentrations in a significantly shorter reaction time using catalyst with activated Biochar Samples 1 and 3. Two different reaction times (i.e., 3 and 6 hours) were tested for the high temperature/pressure runs using catalyst supported on activated Biochar Sample 3 while the rest of reaction parameters such as alcohol to oil molar ratio, catalyst loading, and temperature/pressure remained constant. Results showed that for the longer reaction time (i.e., 6 hour) lower amount of MO and MLO has been produced compared to that of the shorter reaction time (at 3 hour) as shown in Table 4.7. Couple of the probable reasons for the unexpected decrease in the amount of produced methyl esters at longer reaction times could the degradation reaction or deactivation of catalyst. Degradation temperature of MO and MLO are known to be higher than 217°C (Goodwin and Newsham 1975; Wypych 2008); thus, we do not expect any degraded compounds in the product mixture. However in order to

---

[1] As mentioned in Sections 3.2.4 and 3.3.1, the average values and standard deviations have been calculated based on the results of three different samples from product mixture of one reaction. The reaction was not repeated.

confirm the absence of degraded products, GC/MS (Gas Chromatography/ Mass Spectroscopy, Varian CP-3800 GC, MS-4000) analysis was conducted. As shown in Figure 4.4, the product mixture of 6-hour transesterification run (i.e., red GC chromatogram) showed no additional peaks compared to the 3-hour run (i.e., green GC chromatogram). All detected peaks corresponded to the methyl esters of C:18 fatty acid (i.e., Methyl Oleate, Methyl Linoleate, and Methyl Linolenate). Furthermore, the possibility of catalyst deactivation through the time was studied. Data regarding to the time gap between preparation of catalyst and reaction time is included in Appendix A.3. However, no decisive conclusions have been drawn with respect to the decrease in yield after 6 hours.
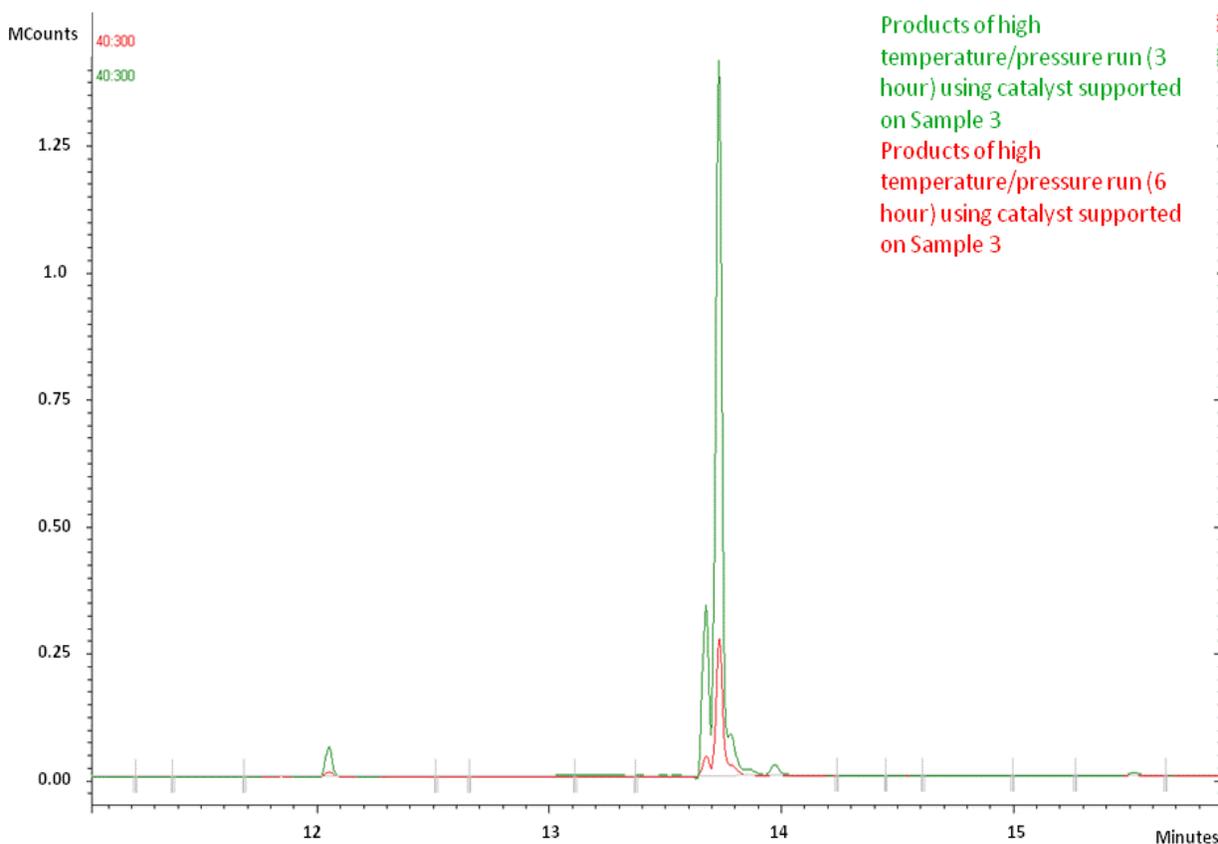
Figure 4.4. GC/MS results for transesterification run under high temperature/pressure

4.5 Structural Study

The unsaturated carbon atoms at the edges of the carbon sheets are available to be functionalized by sulfonation process (Marsh et al. 1997). By constituting larger carbon sheets, the number of available unsaturated carbons from the edges of the carbon sheets is decreased resulting in less available carbons to be functionalized by sulfonation. Consequently, increasing the activation temperature of the support resulted in the reduction of the amount of total acid density of the produced catalyst as evidenced by total acid density and sulfonic group density measurements (Section 4.2.3). Further investigations on the mentioned hypothesis have been conducted through XRD, FT-IR and Elemental Analysis. C-450, C-675 and C-875 represent the activated supports of Biochar Sample 1 at three different temperatures of 450, 675 and 875°C respectively while C-450-SO$_3$H, C-675-SO$_3$H, C-875-SO$_3$H show the corresponding sulfonated catalysts on the activated supports.

4.5.1 XRD spectroscopy

The biochar samples have shown to display disorder towards a specific direction to its carbon sheets known as turbostratic. This is the main reason that the typical XRD patterns of these materials are either considerably broad or absent compared to that of graphite structures (Pierson 1993). However, the presence of narrower definitive peaks of graphite structure (i.e., C(002) and C(101)) in the XRD patterns comparing to the broader ones shows the development of increasingly ordered structure within the carbon network.

The XRD patterns shown in Figures 4.5, 4.6, and 4.7 exhibit similar C(002) diffraction peaks around the 2θ = 15-30° region indicative of an amorphous carbon structure with randomly oriented aromatic carbon sheets (Okamura et al. 2006; Nakajima et al. 2007; Kitano et al. 2009). The narrowing of the C(002) peak as the carbonization temperature increases suggests that higher temperatures result in the formation of a increasingly ordered (i.e., more graphite-like) carbon lattice structure. The definitive C(101) graphite peak around 2θ = 35-50° appears broader and weaker for C-450-SO_3H compared to that of C-675-SO_3H and C-875-SO_3H, again indicating the presence of more graphite-like structures at higher temperatures (Okamura et al. 2006; Nakajima et al. 2007).
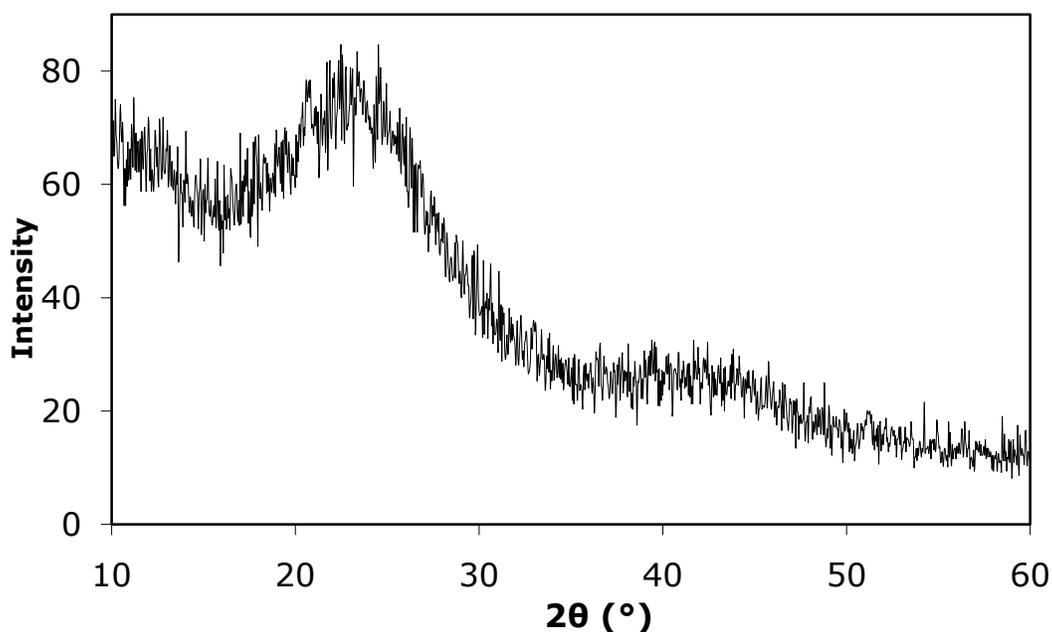
Figure 4.5. XRD pattern of catalyst prepared from char carbonized at 450°C (C-450-SO_3H)
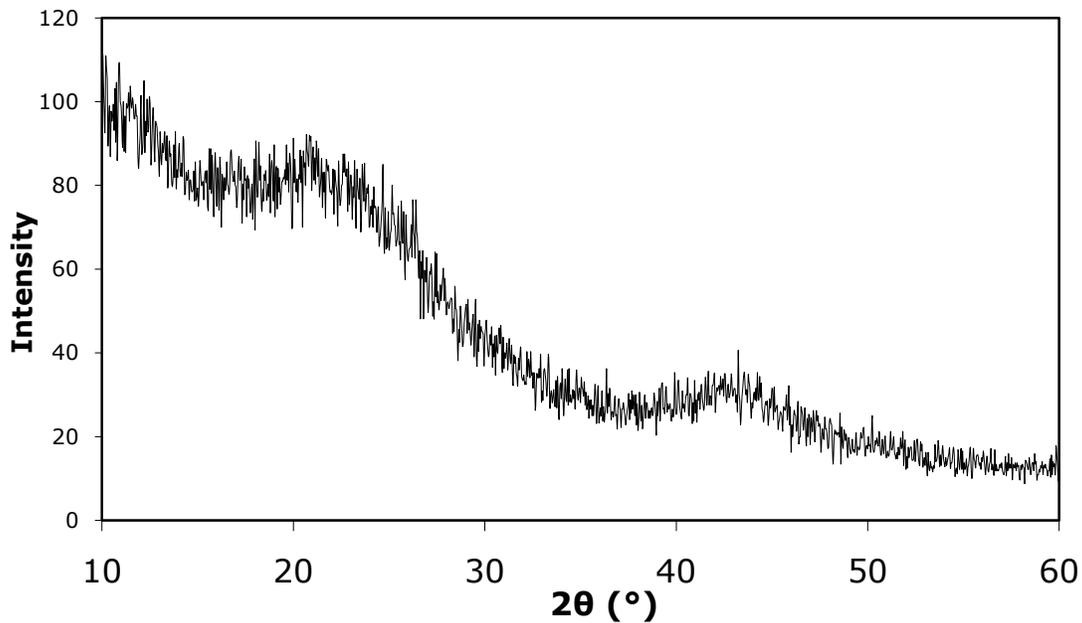
Figure 4.6. XRD pattern of catalyst prepared from char carbonized at 675°C (C-675-SO$_3$H)
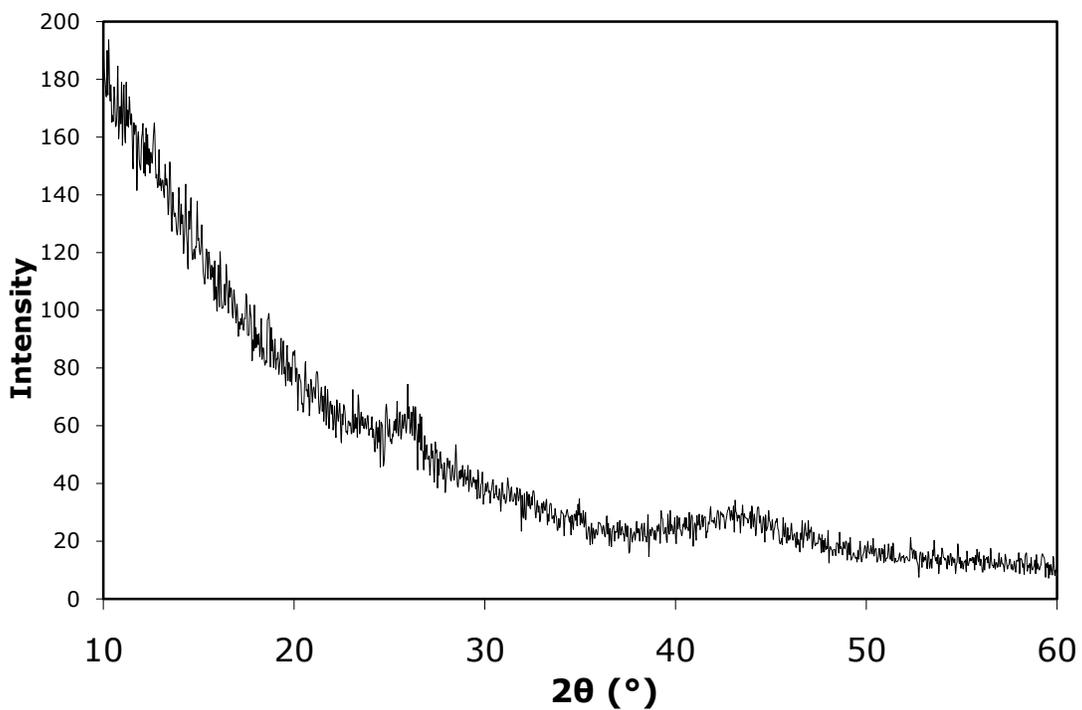
Figure 4.7. XRD pattern of catalyst prepared from char carbonized at 875°C (C-875-SO$_3$H)

4.5.2 FT-IR spectroscopy

Figure 4.8 shows the spectrum for the char activated at 450°C before and after sulfonation. Both spectra contain peaks attributable to aromatic ring modes, at 1581 and 1585 cm^{-1}, respectively (Sharma et al. 2004; Xing et al. 2007; Brewer et al. 2009). Moreover, peaks attributable to C-O-C asymmetric stretching for C-450 and C-450-SO$_3$H can be seen at 1130 and 1150 cm^{-1}, respectively (Zhou et al. 2001). The C-450-SO$_3$H exhibits a peak at 1032 cm^{-1}, which can be attributed to the symmetric S=O stretching (Xing et al. 2007), as well as a peak at 1712 cm^{-1} attributable to the presence of SO$_3$H groups, thereby confirming the incorporation of sulfonic groups onto the carbon matrix after sulfonation (Zong et al. 2007). The C-450 spectrum also has peaks around 1215 cm^{-1} which can be assigned to aromatic acidic (i.e., phenolic) group (Ar-OH stretch) mainly due to oxidization during the carbonization (Xing et al. 2007), and peaks around 1700 cm^{-1} attributable to C=O which are assigned to carboxylic groups (Mo et al. 2008b). However, the peaks attributed to aromatic acidic groups (at 1215 cm^{-1}) and carboxylic groups (at 1700 cm^{-1}) were overlapped in C-450-SO$_3$H spectrum most probably due to the presence of strong sulfonic group peaks.
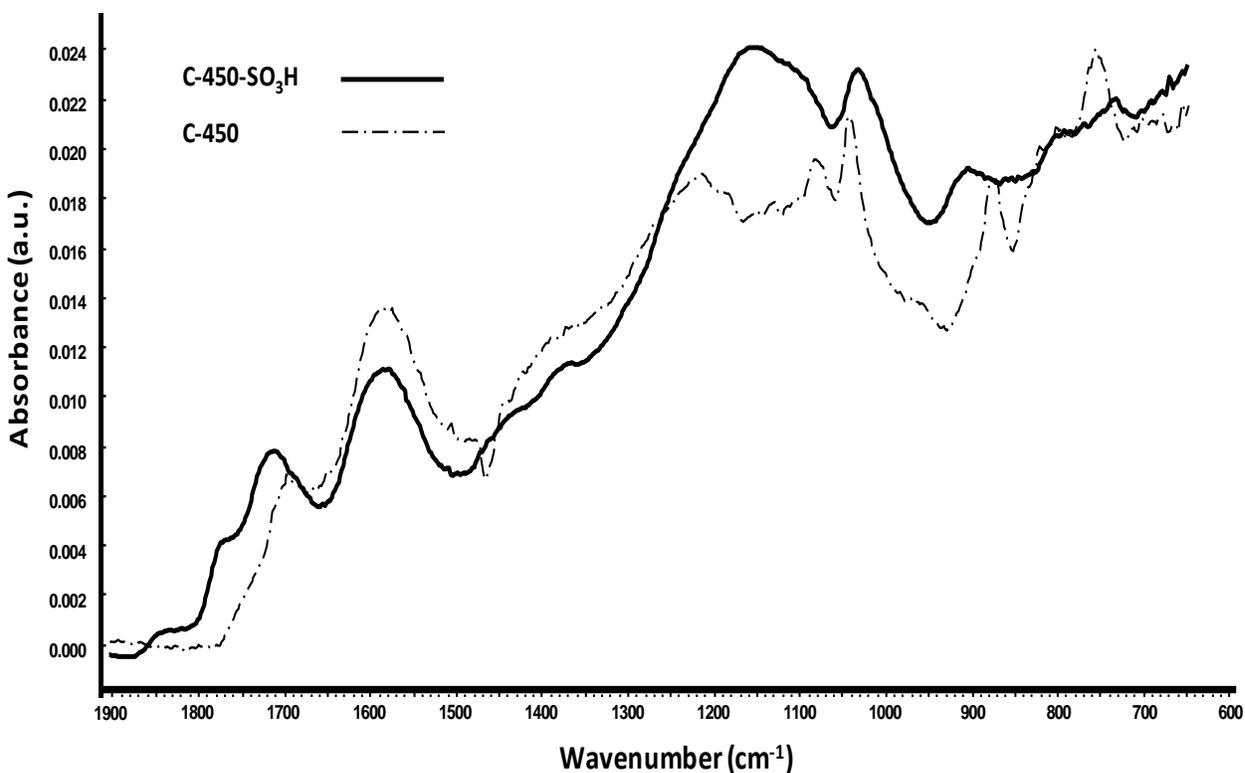
Figure 4.8. FT-IR spectra for catalysts from char carbonized at 450°C before (C-450) and after sulfonation (C-450-SO₃H)

Figure 4.9 shows the FT-IR spectra for chars activated at 450, 675, and 875°C after sulfonation. All three spectra exhibit similar peaks characteristic of the SO_3H groups at 1712, 1717 and 1715 cm^{-1}, respectively, although the peak around 1712 cm^{-1} corresponding to C-450-SO₃H is significantly more intense than that of C-675-SO₃H and C-875-SO₃H. Moreover, the symmetric S=O peak at 1032 cm^{-1} as well as the C-O-C asymmetric stretch at 1150 cm^{-1} present in the C-450-SO₃H is noticeably absent in the latter two spectra confirming the reduction of the total acid density of catalysts through increasing the activation temperature of the support. These results further support the aforementioned hypothesis of decreasing the amount of total acid density through

increasing the activation temperature due to the constitution of larger carbon sheets and essentially more ordered structure.
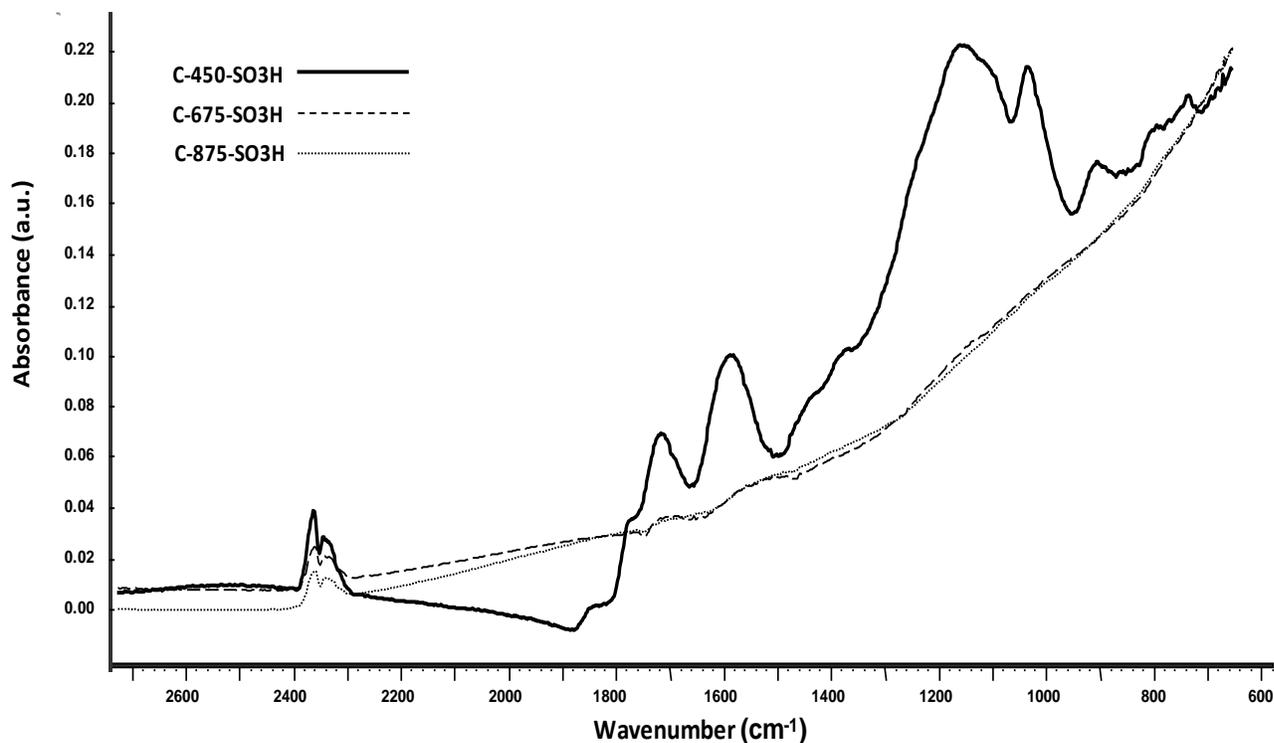
Figure 4.9. FT-IR spectra for catalysts from char carbonized at 450°C (C-450-SO$_3$H), 675°C (C-675-SO$_3$H), and 875°C (C-875-SO$_3$H)

4.5.3 Elemental analysis

The results from the elemental analysis presented in Table 4.9 show a decrease in the H/C and O/C ratios with increasing activation temperature, further supporting the hypothesis that the increasing temperatures cause the evaporation of an increasing number of heteroatoms from the carbon rings resulting in more graphite like structure and more ordering (Lehmann & Joseph 2009). Also, it confirms that by increasing the activation temperature more C-H bonds are ruptured through completing the

carbonization of the support (Thomas & Thomas 1997). In addition, the elemental analysis shows the reduction in sulphur content which confirms the reduction of active sites in the catalyst resulting in decreased total acid density and catalytic activity.

Table 4.9. Elemental Analysis of three different catalysts supported on activated Biochar Sample 1

Char Activation Temperature (°C)	Elemental Analysis Results (%)					H/C	O/C
	C	H	N	O	S		
450	62.64	1.99	<0.3	22.44	2.69	0.005	0.358
675	69.08	<0.3	<0.3	16.24	1.3	0.004	0.235
875	82.39	<0.3	1.01	5.64	1.21	0.004	0.068

5.   General Discussion, Conclusion, and Recommendations

5.1 General Discussion

When the first generation of carbon-based solid acid catalysts was introduced for esterification of FFAs (Toda et al. 2005; Okamura et al. 2006), it was also reported that using activated carbons, carbon blacks and graphitized carbon fibres as catalyst support for esterification and transesterification would not be successful. However, this study showed that using activated carbon from biochar as a support produced a promising catalyst for biodiesel production from either Free Fatty Acids or fresh vegetable oils. Moreover, in the case of carbon-based catalysts from D-glucose precursor it was reported that surface area does not necessarily correlated well with the formation rate, i.e., catalytic activity (Mo et al. 2008a). However, in this study, it was observed that surface area and porosity of the prepared catalysts are important and influential factors on the catalytic activity similar to total acid density and sulfonic group acid density. Nevertheless, preparing biochar-based catalyst from two different biochar samples pyrolyzed from diverse feedstocks (corn stover and softwoods/hardwoods) did not show the same activity as that of the catalyst supported on the biochar sample prepared from wood waste, bark and shavings. However, the catalytic activity has significantly increased while conducting the transesterification reaction at high temperature/pressure conditions.

According to the results of transesterification under high temperature/pressure at two different times using the same catalyst it is postulated that biochar-based catalyst gets deactivated over time, which can be a challenging issue in the development of this

catalyst as a promising candidate for a large scale biodiesel production. However, more investigations on this hypothesis are needed for a stronger conclusion.

5.2. Conclusions

A promising heterogeneous catalyst for biodiesel production has been prepared through sulfonation of biochar, i.e., a by-product of pyrolysis of woody biomass, with fuming sulphuric acid. Biochar is classified as a non-graphitic, non-graphitizable carbon material. Structural study through Elemental Analysis and FT-IR spectroscopy suggests that biochar-based catalyst consists of polycyclic aromatic carbon sheets bearing three different acidic groups of phenolic, carboxylic, and sulfonic. Applying a stronger sulfonation procedure by using stronger sulfonation reagent (fuming vs. concentrated sulphuric acid) and higher mass ratio of sulphuric acid (16.5:1 vs. 10:1) to biochar resulted in higher transesterification activity compared to previous study by West (2006) (~9% yield vs. negligible yield). Further investigations on the biochar-based catalyst have been conducted for the effect of sulfonation time (5 and 15 hours) and surface area development on the transesterification activity. Results show that the catalyst with the highest surface area and acid density, i.e., 2.46 m^2/g and 3.2 mmol/g, respectively, yielded the highest MO and MLO concentrations, i.e., 58.85 and 16.34 g/L, respectively. Furthermore, while the total acid densities are comparable, higher methyl ester concentrations (58.85 vs. 48.32 g/L as MO concentration and 16.34 vs. 13.83 g/L as MLO concentration) are obtained even with a slight increase in the surface area of the catalyst. These results suggest that the surface area and porosity of the biochar-based catalyst are as important factors as the total acid density on transesterification activity.

Thus, the effect of surface area and porosity of biochar-based catalysts on the transesterification activity have been investigated further.

The surface area and porosity of biochar samples have increased via two different methods: silica template, and chemical activation with KOH. In the former method, the pre-formed silica template is mixed with biochar followed by carbonization at 450°C in a tube furnace under nitrogen flow. The activated biochar samples, once the silica template was removed, showed a highly increased surface area and average pore size, 116 m^2/g and 1.97 nm, respectively. The chemical activation technique with KOH involves the reaction of specific amount of biochar with the highly concentrated solution of KOH (7 mol/L) followed by carbonization under nitrogen (258 mL/min) at three temperatures (i.e., 450, 675 and 875°C). The resultant carbonized biochars showed significantly high surface area and porosity as evidenced by pore volume and pore size analysis, i.e., up to 1400 m^2/g, 2.2 nm, and 0.71 cm^3/g for surface area, pore size, and total pore volume, respectively. The carbonized biochars were then sulfonated with fuming sulphuric acid to produce activated biochar-based catalysts. The surface area of the activated biochar samples was drastically reduced upon sulfonation, especially for the biochar sample activated at lowest temperature, i.e., 450°C, which can be attributed to the dissociation of C-C linkage between the loosely bonded carbon sheets of biochar support due to the harsh sulfonation. Three biochar-based catalysts supported on activated biochars at three different temperatures (i.e., 450, 675 and 875°C) were tested for transesterification activity. It was observed that increasing the activation temperature from 450 to 675°C resulted in increased reaction yield to twice of its value (7.6 % vs. 18.9%), likely due to the significant increase in the surface area and pore volume of the

catalyst in spite of decreased amount of total acid density. However, when the activation temperature was further increased to 875°C, instead of the expected increase in catalytic performance, the yield dropped back to about the same value as that obtained for 450°C. This can be explained by the reduced amount of available polycyclic carbons to be functionalized during the sulfonation, and consequently, significant decrease in the amount of total acid density from 1.2 to 0.43 mmol/g. The changes in carbon structure for biochar-based catalysts activated at three different temperatures (i.e., 450, 675 and 875°C) shown through the FT-IR analysis and XRD patterns. Moreover, results of FT-IR and XRD analysis reveal the increasing re-orientation of the carbon sheets into more graphite-like structure as the activation temperature increases, despite of having specific kind of disordering known as turbostratic. By increasing the activation temperature the ratio of C/H has increased and more ordered structure was generated. Through this process the content of available carbons to be functionalized in sulfonation step is reduced and the total acid density has decreased. These results suggest that the catalytic activity of the biochar is dependent on both surface area as well as total acid density and that the maximum would be obtained from an activation temperature, most probably between 675 and 875°C, that would give the optimal condition of the two factors.

The best catalyst based on the highest transesterification yield (18.9 %), i.e., catalyst with activated support at 675°C, were tested for esterification activity of oleic acid using methanol. Results suggest that the mentioned catalyst has considerable activity, i.e., conversion higher than 95%, for esterification process as well as developed transesterification activity.

Since the catalyst supported on chemically activated biochar (i.e., Biochar Sample 1, pyrolyzed from wood waste, white wood, bark and shavings) showed promising results for both transesterification of canola oil and esterification of oleic acid, the same catalyst preparation procedure has been applied to couple of different types of biochar samples pyrolyzed from different raw materials; one from corn stover (Biochar Sample 2) and the other one from hardwoods and softwoods (Biochar Sample 3). All aforementioned biochar-based catalysts have been compared for transesterification activity. Results showed a significant decrease in the amount of reaction yield (18.9 vs. 0.72 and 0,78%) using catalysts supported on Biochar Samples 2 and 3 compared to that of the catalyst supported on Biochar Sample 1, despite of comparable values of surface area and total acid densities of all prepared catalysts. This might be due to the different nature of biochar samples generated from different pyrolysis processes.

Some preliminary transesterification runs at high temperature/pressure conditions (150°C/1.52 MPa) have been conducted using two different biochar-based catalysts supported on biochar Samples 1 and 3. Results suggested that with a similar molar ratio and catalyst loading (15:1 and 5 wt.%, respectively) to atmospheric runs, a higher reaction yield (24.5 vs. 18.9%) can be achieved in a considerably shorter amount of time, i.e., 3 hours vs. 24 hours, using catalyst supported on Biochar Sample 1. Moreover, higher temperature/pressure conditions resulted in considerably higher concentrations of MO and MLO using catalyst supported on activated Biochar Sample 3 in significantly lower amount of time comparing to atmospheric runs (3 or 6 vs. 24 h). However, when comparing results of high temperature/pressure transesterification runs for two different reaction times of 3 and 6 hour, using catalyst supported on Biochar

Sample 3, a decrease in the amount of produced methyl esters was observed (i.e., 156.10 vs. 61.51 g/L as MO concentration and 59.88 vs. 14.86 g/L as MLO concentration). Most likely the catalyst deactivation over time (transesterification runs have been conducted in 1.5 months time gap) may be the possible reason for the difference in the catalytic activities.

5.3. Recommendations for Future Works

The carbon-based catalyst supported on chemically activated biochar showed promising catalytic activity for both transesterification of canola oil and esterification of oleic acid using methanol. Further studies could be performed to determine the reusability as well as their catalytic performance under different reaction conditions, e.g., at higher temperatures and pressures. A suitable experimental design including the investigations of temperature/pressure effect on transesterification activity at different alcohol to oil molar ratios and/or catalyst loading would be useful. The next step would be to combine the FFA feedstock, e.g., oleic acid, with the triglyceride based feedstock, e.g. canola oil, to model the real waste vegetable oil feedstock and to test the simultaneous ability of the biochar-based catalyst for such a feedstock. Based on the results using real waste vegetable oil as feedstock for biodiesel production could be next step. Moreover, modeling a large scale biodiesel production unit using waste vegetable oil and methanol as reaction regents in the presence of biochar-based catalyst and comparison with other well published processes would be beneficial.

For more research works on the development of this catalyst, using stronger functionalizing reagents such as fuming acids with higher percentage of free SO_3 or

super acids is suggested. Moreover, further investigations on the effect of pyrolysis process conditions and feedstock on the catalytic activity of biochar would be useful. .

According to the results of transesterification reaction under high temperature/pressure conditions, catalyst deactivation might be a possible reason for the reduction in the amount of catalytic activity, thus, investigations on this factor should be another important aspects of catalyst development.

Studying the kinetics of transesterification reaction and also finding the optimal temperature which favours all the three reversible consecutive reactions of transesterification (i.e., Triglyceride to Di-Glyceride, Di-Glyceride to Mono-Glyceride, and Mono-Glyceride to Glycerol) would be another interesting aspect of catalyst development.

References

Ahmedna, M., W. E. Marshall, and R. M. Rao. 2000. Surface properties of granular activated carbons from agricultural by-products and their effects on raw sugar decolorization. *Bioresource Technology* 71, no. 2 (January): 103-112. doi:10.1016/S0960-8524(99)90069-X.

Argyropoulos, Dimitris S. 2007. *Materials, Chemicals and Energy from Forest Biomass.* 1st ed. An American Chemical Society Publication, April 16; pp. 469-475.

Azargohar, R., and A.K. Dalai. 2008. Steam and KOH activation of biochar: Experimental and modeling studies. *Microporous and Mesoporous Materials* 110, no. 2-3 (April 15): 413-421. doi:10.1016/j.micromeso.2007.06.047.

Bossaert, Wim D., Dirk E. De Vos, Wim M. Van Rhijn, Joren Bullen, Piet J. Grobet, and Pierre A. Jacobs. 1999. Mesoporous Sulfonic Acids as Selective Heterogeneous Catalysts for the Synthesis of Monoglycerides. *Journal of Catalysis* 182, no. 1 (February 15): 156-164. doi:10.1006/jcat.1998.2353.

Brewer, Catherine E., Klaus Schmidt-Rohr, Justinus A. Satrio, and Robert C. Brown. 2009. Characterization of biochar from fast pyrolysis and gasification systems. *Environmental Progress & Sustainable Energy* 28, no. 3: 386-396. doi:10.1002/ep.10378.

Canakci, M, and H Sanli. 2008. Biodiesel production from various feedstocks and their effects on the fuel properties. *Journal of Industrial Microbiology & Biotechnology* 35, no. 5 (May): 431-41. doi:10.1007/s10295-008-0337-6.

Canakci, M., and J. Van Gerpen. 2001. Biodiesel production from oils and fats with high free fatty acids. *TRANSACTIONS-AMERICAN SOCIETY OF AGRICULTURAL ENGINEERS* 44, no. 6: 1429-1436.

Chen, Xiaoge, S. Jeyaseelan, and N. Graham. 2002. Physical and chemical properties study of the activated carbon made from sewage sludge. *Waste Management* 22, no. 7 (November): 755-760. doi:10.1016/S0956-053X(02)00057-0.

Clark, James H. 2002. Solid Acids for Green Chemistry. *Accounts of Chemical Research* 35, no. 9: 791-797. doi:10.1021/ar010072a.

Demirbas, A. 2003. Chemical and fuel properties of seventeen vegetable oils. *ENERGY SOURCES* 25, no. 7 (July): 721-728. doi:10.1080/00908310390212426.

Demirbas, A., and G. Arin. 2002. An overview of biomass pyrolysis. *Energy Sources, Part A: Recovery, Utilization, and Environmental Effects* 24, no. 5: 471–482.

Dislich, Helmut. 1971. New Routes to Multicomponent Oxide Glasses. *Angewandte Chemie International Edition in English* 10, no. 6: 363-370. doi:10.1002/anie.197103631.

Ertl, Gerhard, H. Knözinger, and Jens Weitkamp. 1999. *Preparation of solid catalysts.* Wiley-VCH;pp. 150-167.

Escobar, José C., Electo S. Lora, Osvaldo J. Venturini, Edgar E. Yáñez, Edgar F. Castillo, and Oscar Almazan. 2009. Biofuels: Environment, technology and food security. *Renewable and Sustainable Energy Reviews* 13, no. 6-7 (8): 1275-1287. doi:10.1016/j.rser.2008.08.014.

Figueiredo, José Luís, Jacob A. Moulijn, and North Atlantic Treaty Organization. Scientific Affairs Division. 1986. *Carbon and coal gasification.* Springer; pp.543-591.

Franklin, R. E. 1951. Crystallite growth in graphitizing and non-graphitizing carbons. *Proceedings of the Royal Society of London. Series A, Mathematical and Physical Sciences*: 196–218.

Goering, C. E, A. W Schwab, M. J Daugherty, E. H Pryde, and A. J Keakin. 1981. *Fuel properties of eleven vegetable oils.*

Goodwin, Stephen R., and David M. T. Newsham. 1975. Kinetics of decomposition of methyl linoleate and vapor-liquid equilibriums in mixtures of methyl palmitate and methyl linoleate. *Journal of Chemical & Engineering Data* 20, no. 2 (April 1): 180-181. doi:10.1021/je60065a026.

Gregg, S. J., and Kenneth S.W. Sing. 1982. *Adsorption, Surface Area, & Porosity, Second Edition.* 2nd ed. Academic Press, February 11.

Gui, M.M., K.T. Lee, and S. Bhatia. 2008. Feasibility of edible oil vs. non-edible oil vs. waste edible oil as biodiesel feedstock. *Energy* 33, no. 11 (November): 1646-1653. doi:10.1016/j.energy.2008.06.002.

Harmer, Mark A., William E. Farneth, and Qun Sun. 1998. Towards the Sulfuric Acid of Solids. *Advanced Materials* 10, no. 15: 1255-1257. doi:10.1002/(SICI)1521-4095(199810)10:15<1255::AID-ADMA1255>3.0.CO;2-T.

Hu, Qingyuan, Jiebin Pang, Zhiwang Wu, and Yunfeng Lu. 2006. Tuning pore size of mesoporous carbon via confined activation process. *Carbon* 44, no. 7 (June): 1349-1352. doi:10.1016/j.carbon.2005.11.021.

Hu, Zhonghua, Huimin Guo, M. P. Srinivasan, and Ni Yaming. 2003. A simple method for developing mesoporosity in activated carbon. *Separation and Purification Technology* 31, no. 1 (April 1): 47-52. doi:10.1016/S1383-5866(02)00148-X.

Hu, Zhonghua, M. P. Srinivasan, and Yaming Ni. 2001. Novel activation process for preparing highly microporous and mesoporous activated carbons. *Carbon* 39, no. 6 (May): 877-886. doi:10.1016/S0008-6223(00)00198-6.

IEA, Medium Term Oil Market Report, © *OECD/IEA, 2009*, Paris.

Khalili, Nasrin R., Marta Campbell, Giselle Sandi, and Janusz Golas. 2000. Production of micro- and mesoporous activated carbon from paper mill sludge: I. Effect of zinc chloride activation. *Carbon* 38, no. 14: 1905-1915. doi:10.1016/S0008-6223(00)00043-9.

Kirakosyan, Ara, and Peter B. Kaufman. 2009. *Recent Advances in Plant Biotechnology*. Springer Dordrecht Heidelberg ,July 9.

Kiss, Anton A., Alexandre C. Dimian, and Gadi Rothenberg. 2006. Solid Acid Catalysts for Biodiesel Production --Towards Sustainable Energy. *Advanced Synthesis & Catalysis* 348, no. 1-2: 75-81. doi:10.1002/adsc.200505160.

Kitano, Masaaki, Keisuke Arai, Atsushi Kodama, Tsutomu Kousaka, Kiyotaka Nakajima, Shigenobu Hayashi, and Michikazu Hara. 2009. Preparation of a Sulfonated Porous Carbon Catalyst with High Specific Surface Area. *Catalysis Letters* 131, no. 1: 242-249. doi:10.1007/s10562-009-0062-4.

Knothe, G. 2001. Historical perspectives on vegetable oil-based diesel fuels. *Inform* 12, no. 11: 1103-1107.

Kulkarni, M. G., R. Gopinath, L. C. Meher, and A. K. Dalai. 2006. Solid acid catalyzed biodiesel production by simultaneous esterification and transesterification. *Green Chemistry* 8, no. 12: 1056-1062.

Lee, J., J. Kim, and T. Hyeon. 2006. Recent Progress in the Synthesis of Porous Carbon Materials. *Advanced Materials* 18, no. 16: 2073-2094. doi:10.1002/adma.200501576.

Lehmann, Johannes, and Stephen Joseph. 2009. *Biochar for environmental management*. Earthscan, May 1.

Lillo-Ródenas, M. A., D. Cazorla-Amorós, and A. Linares-Solano. 2003. Understanding chemical reactions between carbons and NaOH and KOH: An insight into the chemical activation mechanism. *Carbon* 41, no. 2 (February): 267-275. doi:10.1016/S0008-6223(02)00279-8.

Lotero, Edgar, Yijun Liu, Dora E. Lopez, Kaewta Suwannakarn, David A. Bruce, and James G. Goodwin. 2005. Synthesis of Biodiesel via Acid Catalysis. *Industrial & Engineering Chemistry Research* 44, no. 14 (July 1): 5353-5363. doi:10.1021/ie049157g.

Luo, Z., S. Wang, Y. Liao, J. Zhou, Y. Gu, and K. Cen. 2004. Research on biomass fast pyrolysis for liquid fuel* 1. *Biomass and Bioenergy* 26, no. 5: 455–462.

Marsh, Harry, 2001. *Activated carbon compendium*. Gulf Professional Publishing, November 1; pp. x-ix.

Marsh, Harry, Edward A. Heintz, and Francisco Rodríguez-Reinoso. 1997. *Introduction to carbon technologies*. University of Alicante, Secretariado de Publicaciones; pp.35-70.

McNaught, Alan D., and Andrew. Wilkinson. 1997. *Compendium of chemical terminology : IUPAC recommendations / compiled by Alan D. McNaught and Andrew Wilkinson.* Oxford: Blackwell Science.

Melero, Juan A., L. Fernando Bautista, Gabriel Morales, Jose Iglesias, and Rebeca Sánchez-Vázquez. 2010. Biodiesel production from crude palm oil using sulfonic acid-modified mesostructured catalysts. *Chemical Engineering Journal* 161, no. 3 (July 15): 323-331. doi:10.1016/j.cej.2009.12.037.

Mo, Xunhua, Dora E. López, Kaewta Suwannakarn, Yijun Liu, Edgar Lotero, James G. Goodwin Jr., and Changqing Lu. 2008a. Activation and deactivation characteristics of sulfonated carbon catalysts. *Journal of Catalysis* 254, no. 2 (March 10): 332-338. doi:10.1016/j.jcat.2008.01.011.

Mo, Xunhua, Edgar Lotero, Changqing Lu, Yijun Liu, and James Goodwin. 2008b. A Novel Sulfonated Carbon Composite Solid Acid Catalyst for Biodiesel Synthesis. *Catalysis Letters* 123, no. 1 (June 21): 1-6. doi:10.1007/s10562-008-9456-y.

Mohan, Dinesh, Pittman, and Philip H. Steele. 2006. Pyrolysis of Wood/Biomass for Bio-oil: A Critical Review. *Energy & Fuels* 20, no. 3 (May 1): 848-889. doi:10.1021/ef0502397.

Nakajima, Kiyotaka, Michikazu Hara, and Shigenobu Hayashi. 2007. Environmentally Benign Production of Chemicals and Energy Using a Carbon-Based Strong Solid Acid. *Journal of the American Ceramic Society* 90, no. 12: 3725-3734. doi:10.1111/j.1551-2916.2007.02082.x.

Okamura, Mai, Atsushi Takagaki, Masakazu Toda, Junko N. Kondo, Kazunari Domen, Takashi Tatsumi, Michikazu Hara, and Shigenobu Hayashi. 2006. Acid-Catalyzed Reactions on Flexible Polycyclic Aromatic Carbon in Amorphous Carbon. *Chemistry of Materials* 18, no. 13 (June 1): 3039-3045. doi:10.1021/cm0605623.

Okuhara, Toshio. 2002. Water-Tolerant Solid Acid Catalysts. *Chemical Reviews* 102, no. 10 (October 1): 3641-3666. doi:10.1021/cr0103569.

Patrick, John W. 1995. *Porosity in Carbons: Characterization and Applications.* John Wiley & Sons Inc, February; pp. 1-20.

Peng, Li, An Philippaerts, Xiaoxing Ke, Jasper Van Noyen, Filip De Clippel, Gustaaf Van Tendeloo, Pierre A. Jacobs, and Bert F. Sels. 2010. Preparation of sulfonated ordered mesoporous carbon and its use for the esterification of fatty acids. *Catalysis Today* 150, no. 1-2 (February 26): 140-146. doi:10.1016/j.cattod.2009.07.066.

Pierson, Hugh O. 1993. *Handbook of carbon, graphite, diamond, and fullerenes.* William Andrew; pp. 70-84.

Raymundo-Piñero, E., P. Azaïs, T. Cacciaguerra, D. Cazorla-Amorós, A. Linares-Solano, and F. Béguin. 2005. KOH and NaOH activation mechanisms of multiwalled carbon nanotubes with different structural organisation. *Carbon* 43, no. 4: 786-795. doi:10.1016/j.carbon.2004.11.005.

Reed, S. J. B. 2005. *Electron microprobe analysis and scanning electron microscopy in geology.* Cambridge University Press.

Rodríguez-Reinoso, F., and M. Molina-Sabio. 1998. Textural and chemical characterization of microporous carbons. *Advances in Colloid and Interface Science* 76-77 (July 1): 271-294. doi:10.1016/S0001-8686(98)00049-9.

Sakka, Sumio, and Kanichi Kamiya. 1980. Glasses from metal alcoholates. *Journal of Non-Crystalline Solids* 42, no. 1-3 (October): 403-421. doi:10.1016/0022-3093(80)90040-X.

Sejidov, Firdovsi Tataroglu, Yagoub Mansoori, and Nadereh Goodarzi. 2005. Esterification reaction using solid heterogeneous acid catalysts under solvent-less condition. *Journal of Molecular Catalysis A: Chemical* 240, no. 1-2 (October 3): 186-190. doi:10.1016/j.molcata.2005.06.048.

Sharma, Ramesh K., Jan B. Wooten, Vicki L. Baliga, Xuehao Lin, W. Geoffrey Chan, and Mohammad R. Hajaligol. 2004. Characterization of chars from pyrolysis of lignin. *Fuel* 83, no. 11-12 (August): 1469-1482. doi:10.1016/j.fuel.2003.11.015.

Shimada, Yuji, Yomi Watanabe, Taichi Samukawa, Akio Sugihara, Hideo Noda, Hideki Fukuda, and Yoshio Tominaga. 1999. Conversion of vegetable oil to biodiesel using immobilized Candida antarctica lipase. *Journal of the American Oil Chemists' Society* 76, no. 7 (July 1): 789-793. doi:10.1007/s11746-999-0067-6.

Sipilae, K., E. Kuoppala, L. Fagern\äs, and A. Oasmaa. 1998. Characterization of biomass-based flash pyrolysis oils. *Biomass and Bioenergy* 14, no. 2: 103–113.

Suppes, Galen J., Mohanprasad A. Dasari, Eric J. Doskocil, Pratik J. Mankidy, and Michael J. Goff. 2004. Transesterification of soybean oil with zeolite and metal catalysts. *Applied Catalysis A: General* 257, no. 2 (January 20): 213-223. doi:10.1016/j.apcata.2003.07.010.

Supple, B., R. Howard-Hildige, Esther Gonzalez-Gomez, and J. Leahy. 2002. The effect of steam treating waste cooking oil on the yield of methyl ester. *Journal of the American Oil Chemists' Society* 79, no. 2 (February 1): 175-178. doi:10.1007/s11746-002-0454-1.

Takagaki, Atsushi, Masakazu Toda, Mai Okamura, Junko N. Kondo, Shigenobu Hayashi, Kazunari Domen, and Michikazu Hara. 2006. Esterification of higher fatty acids by a novel strong solid acid. *Catalysis Today* 116, no. 2 (August 1): 157-161. doi:10.1016/j.cattod.2006.01.037.

Thomas, John Meurig, and W. J. Thomas. 1997. *Principles and practice of heterogeneous catalysis*. Wiley-VCH; pp. 319-380.

Toda, Masakazu, Atsushi Takagaki, Mai Okamura, Junko N. Kondo, Shigenobu Hayashi, Kazunari Domen, and Michikazu Hara. 2005. Green chemistry: Biodiesel made with sugar catalyst. *Nature* 438, no. 7065 (November 10): 178. doi:10.1038/438178a.

Webb, Paul A., and Clyde Orr. 1997. *Analytical Methods in Fine Particle Technology*. 1st ed. Micromeritics Instrument Corporation, March.

West, A.H., 2006. Process simulation and catalyst development for biodiesel production. Thesis, (MASc). University of British Columbia

West, Alex H., Dusko Posarac, and Naoko Ellis. 2008. Assessment of four biodiesel production processes using HYSYS.Plant. *Bioresource Technology* 99, no. 14 (September): 6587-6601. doi:10.1016/j.biortech.2007.11.046.

Wypych, George, 2008. *Knovel Solvents - A Properties Database.* ChemTec Publishing. Online version available at:
http://knovel.com/web/portal/browse/display?_EXT_KNOVEL_DISPLAY_bookid=635&VerticalID=0

Xing, Rong, Yueming Liu, Yong Wang, Li Chen, Haihong Wu, Yongwen Jiang, Mingyuan He, and Peng Wu. 2007. Active solid acid catalysts prepared by sulfonation of carbonization-controlled mesoporous carbon materials. *Microporous and Mesoporous Materials* 105, no. 1-2 (September 15): 41-48. doi:10.1016/j.micromeso.2007.06.043.

Yaman, S. 2004. Pyrolysis of biomass to produce fuels and chemical feedstocks. *Energy Conversion and Management* 45, no. 5: 651–671.

Yoldas, B. E. 1979. Monolithic glass formation by chemical polymerization. *Journal of Materials Science* 14, no. 8: 1843-1849. doi:10.1007/BF00551023.

Zhang, Y., M. A. Dubé, D. D. McLean, and M. Kates. 2003. Biodiesel production from waste cooking oil: 2. Economic assessment and sensitivity analysis. Bioresource Technology 90, no. 3 (December): 229-240. doi:10.1016/S0960-8524(03)00150-0.

Zhou, Weiliang, Makoto Yoshino, Hidetoshi Kita, and Ken-ichi Okamoto. 2001. Carbon Molecular Sieve Membranes Derived from Phenolic Resin with a Pendant Sulfonic Acid Group. Industrial *& Engineering Chemistry Research* 40, no. 22 (October 1): 4801-4807. doi:10.1021/ie010402v.

Zong, Min-Hua, Zhang-Qun Duan, Wen-Yong Lou, Thomas J. Smith, and Hong Wu. 2007. Preparation of a sugar catalyst and its use for highly efficient production of biodiesel. *Green Chemistry* 9, no. 5: 434-437.

Appendices

A.1 Effect of Higher Amount of HCL in Formation of Silica Template

As mentioned in Section 3.2.1, to form the silica template the molar ratio of TEOS: H2O: Ethanol: HCL should be set to (1:6:6:0.01) according to the method of (Q. Hu et al. 2006). However, in the first run, the amount of HCL was incorrectly set to (0.9204 g) instead of (0.0915 g) so the molar ratio of TEOS: H2O: Ethanol: HCL has been changed to (1:6:6:0.1) instead of (1:6:6:0.01). According to the literature (Kawashima et al. 2000), since HCL plays the catalyst role for sol-gel process, higher HCL content results in higher degree of polymerization and consequently more surface area of the activated biochar via silica template method. Table A.1 shows the BET results of the two activated biochars prepared from different silica templates.

Table A.1. Surface area and Porosity Characterization of activated biochar via two different prepared silica templates

Sample	TEOS:H_2O:Ethanol: HCL ratio	BET surface area (m^2/g)	Pore Size (nm)	Total Pore volume (cm^3/g)
Activated Biochar on Silica Template 1	1:6:6:0.01	86.8	1.99	0.034
Activated Biochar on Silica Template 2	1:6:6:0.1	116	1.97	0.046

Since the activated biochar on Silica template 2 resulted in higher BET surface area, it has been reported in the results and discussion of this thesis.

A.2 Detailed Steps of Chemical Activation Method

```
┌─────────────────────────────────────────┐
│        Biochar was crushed and           │
│   sieved to: -250µm +38µm and            │
│   dried at 120°C for 2:30 h in           │
│              oven                        │
└─────────────────────────────────────────┘
                    ⇩
┌─────────────────────────────────────────┐
│ KOH solution (7 mol/L) has been prepared │
│ using KOH pellets (containing 10-15%     │
│ water) and distilled water               │
└─────────────────────────────────────────┘
                    ⇩
┌─────────────────────────────────────────┐
│ 150 mL of KOH solution (7 mol/L) was     │
│ mixed with specified amount of biochar   │
│ and stirred at room temperature for 2 h  │
└─────────────────────────────────────────┘
                    ⇩
┌─────────────────────────────────────────┐
│ After filtration, the treated biochar    │
│ was dried at 120°C over night            │
└─────────────────────────────────────────┘
                    ⇩
┌─────────────────────────────────────────┐
│ 10 g of prepared biochar sample is       │
│ placed in tube furnace (1st step:        │
│ ramping rate 3°C/min to 300°C, dwell     │
│ time: 1h, 2nd step: ramping rate 3°C/min │
│ to desired temperature, dwell time 2h)   │
│ under nitrogen flow (258 mL/min)         │
└─────────────────────────────────────────┘
                    ⇩
┌─────────────────────────────────────────┐
│ Treatment with 0.1 M HCL followed by     │
│ deionized water until pH of wash water   │
│ turns neutral                            │
└─────────────────────────────────────────┘
                    ⇩
         Drying at 110°C for 12h
```
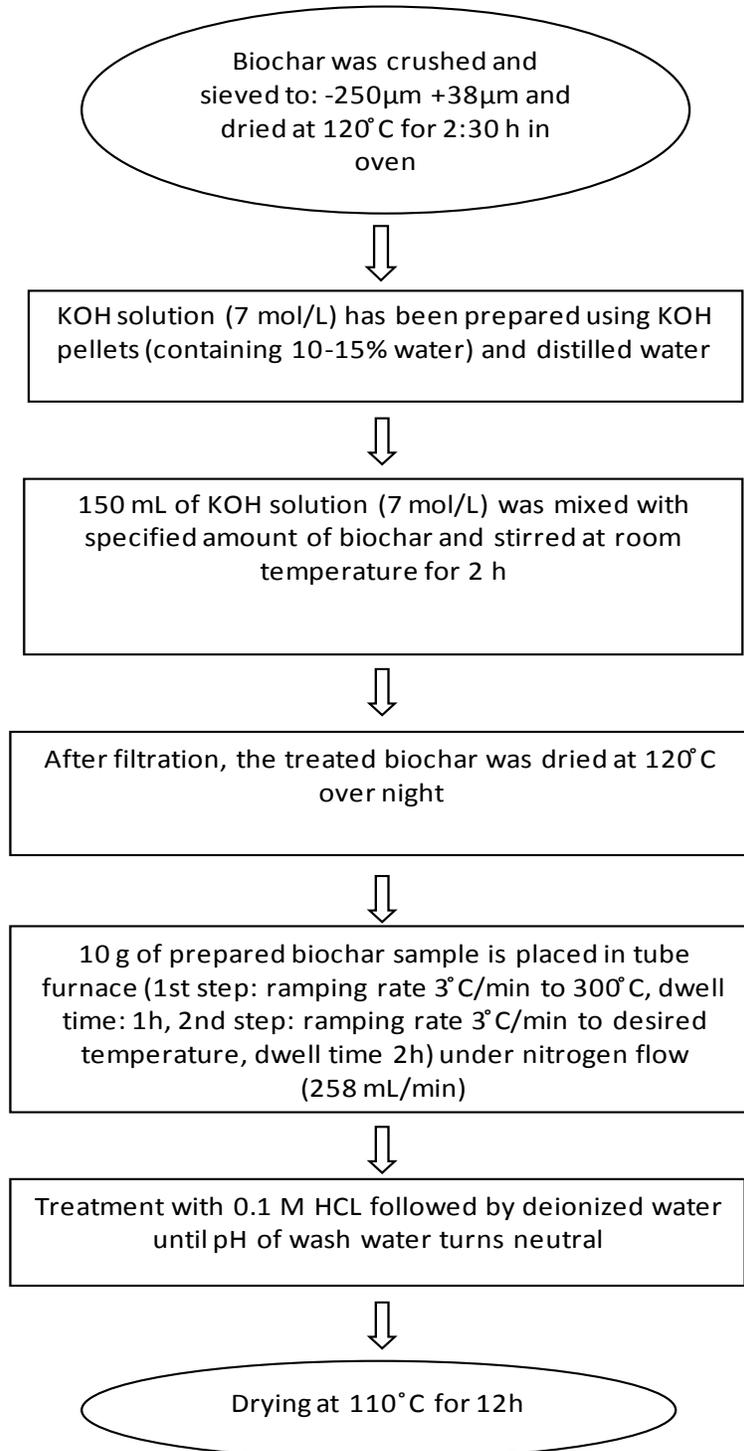
Figure A.1. Chemical activation process via KOH

A.3 Effect of Time on Catalytic Activity of Transesterification in Autoclave Runs

As shown in Table A.2, in all cases of transesterification runs under high temperature/pressure conditions, there is at least 2.5 months time gap between preparation date of catalyst and the date that transesterification run has been conducted. Also, it can be seen that using the same catalyst with same reaction parameters such as alcohol to oil molar ratio, reaction temperature/pressure, and catalyst loading resulted in less produced amounts of methyl esters when extending the reaction time from 3 to 6 hour. Since, the transesterification is a reversible reaction by extending the reaction time at least the concentration of products should be remained constant, while data in Table A.2 suggest contrary results. One of the possible reasons for the unexpected results might be due to the deactivation of catalyst over time, however, further investigations on this topic were not possible due to the limitations of time.

Another unexpected result was the amount of increase in the catalytic activity of the catalyst supported on Biochar Sample 1 comparing to Sample 3 as evidenced by the amount of MO and MLO concentrations. As shown in table A.2, conducting the transesterification reaction under high temperature/pressure conditions using the catalyst supported on Biochar Sample 3 resulted in an increase by almost 70 times comparing to atmospheric run, while the same amount was remained almost the same for the catalyst supported on Biochar Sample 1. Once again, a possible reason for this

unexpected result might be due to the deactivation of catalyst (i.e., supported on sample

1) over time (6 months).

Table A.2. Time gaps between preparation and testing dates of biochar based catalyst under high temperature/pressure transesterification

Catalyst Sample	Reaction Conditions[1] (Temperature /Pressure, Time)	Approximate time gap between preparation of catalyst and transesterification run	MO concentration (g/L)	MLO concentration (g/L)	Reaction Yield (%)
Supported on Activated Biochar Sample 3 at 675°C	150°C/1.52 MPa, 3 h	2.5 months	156.10±13.43	59.88±5.02	-
	150°C/1.52 MPa, 6 h	3.5 months	61.51±3.18	14.86±0.76	-
	150°C/1.52 MPa, 6 h	3.5 months	42.28±2.77	10.78±0.89	-
	65°C/ atmospheric, 24 h	1 week	3.97±0.36	0.82±0.37	0.78±0.08
Supported on activated Biochar Sample 1 at 675°C	150°C/1.52 MPa, 3 h	6 months	113.28 ± 2.95	33.24±0.88	24.5±0.5
	65°C/ atmospheric, 24 h	1 week	124.71±4.65	33.24±1.23	18.9±0.6

---

[1] All reaction conditions except for temperature/pressure and time were maintained constant, i.e., alcohol to oil molar ratio 15:1 and catalyst loading 5 wt.% based on canola oil.